Probing electroweak baryogenesis induced by extra bottom Yukawa coupling via EDMs and collider signatures

Tanmoy Modak[a,b] **and Eibun Senaha**[c,d]

[a]*Department of Physics, Osaka University,*
Toyonaka, Osaka 560-0043, Japan

[b]*Department of Physics, National Taiwan University,*
Taipei 10617, Taiwan

[c]*Theoretical Particle Physics and Cosmology Research Group,*
Advanced Institute of Materials Science, Ton Duc Thang University,
Ho Chi Minh City, Vietnam

[d]*Faculty of Applied Sciences, Ton Duc Thang University,*
Ho Chi Minh City, Vietnam

E-mail: tanmoyy@gmail.com, eibun.senaha@tdtu.edu.vn

ABSTRACT: We study the prospect of probing electroweak baryogenesis driven by an extra bottom Yukawa coupling ρ_{bb} in a general two Higgs doublet model via electric dipole moment (EDM) measurements and at the collider experiments. The parameter space receives meaningful constraints from $125\,\mathrm{GeV}$ Higgs h boson signal strength measurements as well as several heavy Higgs boson searches at the Large Hadron Collider (LHC). In addition, we show that the asymmetry of the CP asymmetry of inclusive $B \to X_s\gamma$ decay would provide complementary probe. A discovery is possible at the LHC via $bg \to bA \to bZh$ process if $|\rho_{bb}| \sim 0.15$ and $250\,\mathrm{GeV} \lesssim m_A \lesssim 350\,\mathrm{GeV}$, where A is CP odd scalar. For $m_A > 2m_t$ threshold, where m_t is the top quark mass, one may also discover $bg \to bA \to bt\bar{t}$ at the high luminosity LHC run if an extra top Yukawa coupling $|\rho_{tt}| \sim 0.5$, though it may suffer from systematic uncertainties. For completeness we study $gg \to t\bar{t}A \to t\bar{t}b\bar{b}$ but find it not promising.

KEYWORDS: Beyond Standard Model, CP violation, Heavy Quark Physics, Higgs Physics

Contents

1 Introduction

The existence of the matter-antimatter asymmetry is unswervingly established over the years by various cosmological observations such as the cosmic microwave background anisotropies and big-bang nucleosynthesis [1]. It has been understood that the Universe started with equal number of baryons and antibaryons, but later evolved into baryon dominated Universe dynamically via a mechanism called baryogenesis. A successful baryogenesis requires three necessary conditions namely, baryon number violation, charge conjugation (C) and charge conjugation-parity (CP) violation and, departure from thermal equilibrium, laid out by Sakharov in 1967 [2]. A plethora of baryogenesis scenarios have been proposed so far to account for the observed baryon asymmetry of the Universe (BAU), however, its origin is still unclear. After the discovery of the 125 GeV Higgs boson at the Large Hadron Collider (LHC) [3], a significant attention has been directed in particular to electroweak baryogenesis (EWBG) [4, 15–89][1] mechanism for its direct connections to Higgs physics and, its testability at the ongoing experiments. The Standard Model (SM) belongs to this class, however the CP violation is too small and, the electroweak symmetry breaking is not strongly first order phase transition (EWPT) to drive departure from thermal equilibrium.

While we do not have any strong experimental evidence of new physics yet, multi-Higgs sector is the natural consequence of most ultraviolet (UV) theories due to enlarged

---

[1]For some reviews see e.g. refs. [5–14].

symmetries. Whatever the fundamental theory might be, their effective descriptions at $\mathcal{O}(100)\,\text{GeV}$ scale should resemble the SM in light of the latest experimental results. As for the Higgs sector, two cases are conceivable: one is that all the new scalars are much heavier than $\mathcal{O}(100)\,\text{GeV}$ scale, thereby the Higgs sector is effectively reduced to the SM, while the other is that new scalars have $\mathcal{O}(100)\,\text{GeV}$ masses but their couplings to the gauge bosons and fermions are SM like, mimicking the SM. From the viewpoint of new physics discovery potential, it is timely to consider the latter case and investigate whether the aforementioned cosmological issue can be solved or not. Since we have already confirmed the existence of the Higgs doublet in nature, it is tempting to us to think of additional Higgs doublets in analogy with the fact that all the fermions come in three copies.

The general two Higgs doublet model (g2HDM) is one of the simplest renormalizable low-energy models where the scalar sector of the SM is extended by an extra scalar doublet.[2] Without the presence of discrete symmetry, in g2HDM, both the scalar doublets couple with up- and down-type fermions at tree level. In the mass eigenbasis of the fermions (F), one has two independent Yukawa couplings λ_{ij}^F and ρ_{ij}^F, where the former is real and diagonal that are responsible for the fermion mass generation, while the latter is complex and non-diagonal. Such complex couplings can provide additional CP violating sources beyond the usual Cabibbo-Kobayashi-Maskawa (CKM) framework [92] of the SM.

EWBG in g2HDM is widely investigated in refs. [79–86]. This model can simultaneously accommodate the strong first-order EWPT and sufficient amount of CP violation which the SM fails to provide. The most natural EWBG scenario in g2HDM would be the case in which BAU is driven by the extra top Yukawa coupling (ρ_{tt}) of $\mathcal{O}(0.01-1)$ in magnitude with moderate size of the CP phase (ρ_{tt}-EWBG) [84]. The devoted collider study of this scenario is conducted in ref. [93].

As a complementary study to ρ_{tt}-EWBG, the present authors consider a scenario in which the CP phase of ρ_{tt} is approximately zero and the extra bottom Yukawa coupling (ρ_{bb}) plays a dominant role in generating BAU (ρ_{bb}-EWBG) [85]. It is demonstrated that BAU can reach the observed level if $|\text{Im}\rho_{bb}| \gtrsim 0.058$ with generous assumptions on a Higgs bubble wall profile. There exist several direct and indirect search constraints on the parameter space for ρ_{bb}-EWBG such as h boson signal strength measurements, heavy Higgs searches at the LHC. The ρ_{bb}-EWBG can be discovered at the LHC via $bg \to bA \to bZH$ (or $bg \to bH \to bZA$) process if $|\text{Im}(\rho_{bb})| \sim \mathcal{O}(0.1)$ [94]. However, the process requires that $m_A > m_H + m_Z$ and ρ_{tt} to be negligibly small to avoid constraints from flavor physics [94]. In addition, for $m_A > 2m_t$, the process gets dilution from $A \to t\bar{t}$ decay if ρ_{tt} is nonvanishing. Also, it would be extremely difficult to probe the phase of ρ_{bb} at the LHC since its information is lost in pp collision.

In this paper we show that the electron EDM measurement and asymmetry of CP asymmetry of the $B \to X_s\gamma$ decay offer exquisite probes for $\text{Im}(\rho_{bb})$. We also analyze the prospect of discovery at the LHC. In particular we study the discovery potential of ρ_{bb}-EWBG via $bg \to bA \to bZh$ and $bg \to bA \to bt\bar{t}$ processes at $14\,\text{TeV}$ LHC. Purpose of this paper is to find possible direct and indirect signatures and correlation between them in probing the parameter space for the ρ_{bb}-EWBG.

---

[2]For pedagogical reviews on 2HDM see e.g. refs. [90, 91] and references there in.

Induced by ρ_{bb}, the $bg \to bA \to bZh$ process can be searched at the LHC via $pp \to bA + X \to bZh + X$ (X is inclusive activities) followed by $Z \to \ell^+\ell^-$ ($\ell = e,\ \mu$) and $h \to b\bar{b}$ decays, constituting same flavor opposite sign dilepton pair and three b-tagged jets. While the $bg \to bA \to bZh$ process can be induced ρ_{bb}, the $bg \to bA \to bt\bar{t}$ process requires both ρ_{bb} and ρ_{tt} to be nonvanishing. The latter process can be searched via $pp \to bA + X \to bt\bar{t} + X$ with at least one top decays semileptonically, constituting three b-tagged jets, at least one charged lepton (e and μ) and missing transverse energy signature (denoted as $3b1\ell$ process). These processes provide the sensitive probes for the parameter space of ρ_{bb}-EWBG, which is complementary to ref. [94].

For the sake of completeness we also investigate the discovery prospect of the $gg \to t\bar{t}A \to t\bar{t}b\bar{b}$ process, which is induced by nonzero ρ_{bb} and ρ_{tt}. At the LHC the process can be searched via $pp \to t\bar{t}A + X \to t\bar{t}b\bar{b} + X$, with at least one top decaying semileptonically. As ρ_{tt} gets involved in both $bg \to bA \to bt\bar{t}$ and $gg \to t\bar{t}A \to t\bar{t}b\bar{b}$, the processes would provide complementary probes also for ρ_{tt}-EWBG.

In the following, we outline the formalism in section 2, followed by a detailed discussion on the available parameter space and potential indirect probes in section 3. We discuss the discovery potential of ρ_{bb}-EWBG at the LHC in section 4 and summarize our results with some outlook in section 5.

2 Framework

The particle content of g2HDM is the SM plus additional Higgs doublet. In general, this model induces flavor-changing neutral current (FCNC) processes mediated by the neutral Higgs bosons at tree level. It is common to impose a Z_2 symmetry to suppress the FCNC processes to be consistent with various flavor physics data. Though this setup works well, having the Z_2 symmetry implies that the model has some specific UV theories such as supersymmetric models. Since we do not try to connect the model to any specific UV completions, we do not impose the Z_2 symmetry or something similar, which enables us to discuss physics at $\mathcal{O}(100)\,\mathrm{GeV}$ scale in wider perspective. In this bottom-up approach, the tree-level FCNC processes are possible as long as the experimental data allow, and sources of CP violation are much richer than 2HDMs with some discrete symmetries.

The most general two Higgs doublet potential can be written in the Higgs basis as [95, 96]

$$
V(\Phi, \Phi') = \mu_{11}^2 |\Phi|^2 + \mu_{22}^2 |\Phi'|^2 - (\mu_{12}^2 \Phi^\dagger \Phi' + \mathrm{H.c.}) + \frac{\eta_1}{2}|\Phi|^4 + \frac{\eta_2}{2}|\Phi'|^4 + \eta_3 |\Phi|^2 |\Phi'|^2
$$
$$
+ \eta_4 |\Phi^\dagger \Phi'|^2 + \left[\frac{\eta_5}{2}(\Phi^\dagger \Phi')^2 + \left(\eta_6 |\Phi|^2 + \eta_7 |\Phi'|^2 \right) \Phi^\dagger \Phi' + \mathrm{H.c.} \right]. \tag{2.1}
$$

Each Higgs doublet fields is expressed as

$$
\Phi = \begin{pmatrix} G^+ \\ \frac{1}{\sqrt{2}}(v + h + iG^0) \end{pmatrix}, \quad \Phi' = \begin{pmatrix} H^+ \\ \frac{1}{\sqrt{2}}(A + H) \end{pmatrix}, \tag{2.2}
$$

where $v(\simeq 246$ GeV$)$ is the vacuum expectation value, h is the SM-like Higgs boson, $G^{0,\pm}$ are the Nambu-Goldstone bosons, H and A are the CP-even and -odd Higgs bosons, respectively, and $H^\pm$ are the charged Higgs bosons. From the minimization condition with respect to Φ, it follows that $\mu_{11}^2 = -\eta_1 v^2/2$. For simplicity, we assume CP-conserving Higgs sector at tree level.[3] The second minimization condition with respect to Φ' gives $\mu_{12}^2 = \eta_6 v^2/2$.

The mixing angle γ between the CP-even bosons h and H satisfies the relations [96]

$$\cos^2\gamma = \frac{\eta_1 v^2 - m_h^2}{m_H^2 - m_h^2}, \qquad \sin 2\gamma = \frac{2\eta_6 v^2}{m_H^2 - m_h^2}. \tag{2.3}$$

An alignment limit is defined as $c_\gamma = 0$ and $s_\gamma = -1$, where c_γ and s_γ are shorthands for $\cos\gamma$ and $\sin\gamma$ respectively. One can express the masses of h, H, A and $H^\pm$ in terms of the parameters in eq. (2.1):

$$m_{h,H}^2 = \frac{1}{2}\left[m_A^2 + (\eta_1 + \eta_5)v^2 \mp \sqrt{\left[m_A^2 + (\eta_5 - \eta_1)v^2\right]^2 + 4\eta_6^2 v^4} \right], \tag{2.4}$$

$$m_A^2 = \frac{1}{2}(\eta_3 + \eta_4 - \eta_5)v^2 + \mu_{22}^2, \tag{2.5}$$

$$m_{H^\pm}^2 = \frac{1}{2}\eta_3 v^2 + \mu_{22}^2. \tag{2.6}$$

Note that in the alignment limit, one has $m_h^2 = \eta_1 v^2$ and $m_H^2 = m_A^2 + \eta_5 v^2 = (\eta_3 + \eta_4 + \eta_5)v^2/2 + \mu_{22}^2$. In contrast to m_h, the masses of the extra Higgs bosons are controlled by $\eta_i v^2$ and μ_{22}^2, where η_i denotes some linear combinations of the η couplings. As is well known, magnitudes of the heavy Higgs loop contributions can become sizable if $\eta_i v^2 \gtrsim \mu_{22}^2$, which is necessary for achieving the strong first-order EWPT.

The CP-even scalars h, H and CP-odd scalar A couple to fermions by [95]

$$\mathcal{L} = -\frac{1}{\sqrt{2}} \sum_{F=U,D,L} \bar{F}_i \left[(-\lambda_{ij}^F s_\gamma + \rho_{ij}^F c_\gamma)h + (\lambda_{ij}^F c_\gamma + \rho_{ij}^F s_\gamma)H - i\,\mathrm{sgn}(Q_F)\rho_{ij}^F A \right] P_R F_j$$

$$- \bar{U}_i \left[(V\rho^D)_{ij} P_R - (\rho^{U\dagger}V)_{ij} P_L \right] D_j H^- \bar{\nu}_i \rho_{ij}^L P_R L_j H^+ + \text{H.c.}, \tag{2.7}$$

where $P_{L,R} \equiv (1 \mp \gamma_5)/2$, $i,j = 1,2,3$ are generation indices, V is CKM matrix, and $U = (u,c,t)$, $D = (d,s,b)$, $L = (e,\mu,\tau)$ and $\nu = (\nu_e, \nu_\mu, \nu_\tau)$ are in vectors in flavor space. The matrices λ_{ij}^F $(= \sqrt{2}m_i^F/v)$ are real and diagonal, whereas ρ_{ij}^F are in general complex and non-diagonal.

Purpose of this paper is to probe the parameter space for EWBG driven by the extra bottom Yukawa ρ_{bb}. It is found that a successful EWBG requires $|\mathrm{Im}(\rho_{bb})| \gtrsim 0.058$ [85]. In the following we shall show that the parameter space receives meaningful constraints from several direct and indirect searches. The most stringent constraint on $\mathrm{Im}(\rho_{bb})$ arises from electron EDM and $\Delta\mathcal{A}_{\mathrm{CP}}$ of $\mathcal{B}(B \to X_s\gamma)$. In addition, coupling strength measurements of h and heavy Higgs searches at the LHC would also provide the complementary probes. In

---

[3]Since we have CP violation in the Yukawa sector as delineated below, its effect appears in the Higgs spectrum at one-loop level and CP-even and -odd Higgs boson mix with each other. Nevertheless, such a one-loop induced mixing is so small that $\{h, H, A\}$ can be regarded as the mass eigenstates to a good approximation.

addition to these constraints, we also study potential signatures at the LHC. We primarily focus on three searches at the 14 TeV LHC $bg \to bA \to bZh$,[4] $gg \to t\bar{t}A \to t\bar{t}b\bar{b}$ and $bg \to bA \to bt\bar{t}$ (for the discussion on latter two processes see also refs. [105][5]). Induced by ρ_{bb} the $bg \to bA \to bZh$ process can be searched at the LHC if c_γ is nonzero and $m_A > m_h + m_Z$. On the other hand, $gg \to t\bar{t}A \to t\bar{t}b\bar{b}$ process requires ρ_{tt} and ρ_{bb} both nonvanishing with mild dependence on c_γ. The final process $bg \to bA \to bt\bar{t}$ also depends both on ρ_{bb} and ρ_{tt} but needs $m_A > 2m_t$. Together with electron EDM and $\Delta\mathcal{A}_{\rm CP}$ of $\mathcal{B}(B \to X_s\gamma)$, these processes can probe significant part of the parameter space for ρ_{bb}-EWBG.

Note that complex ρ_{tt} can provide a more robust mechanism for EWBG [84, 86]. One may also have complementary probes for the ρ_{tt}-EWBG from $gg \to t\bar{t}A \to t\bar{t}b\bar{b}$ and $bg \to bA \to bt\bar{t}$ processes. Nonvanishing ρ_{tt} motivates the conventional $gg \to H \to t\bar{t}$ [106, 107][6] search or $gg \to t\bar{t}A/H \to t\bar{t}t\bar{t}$ [101–105],[7] i.e., the four top search. Though the former process suffers from large interference with the overwhelming QCD $gg \to t\bar{t}$ background [108], recent searches performed by both ATLAS [106] and CMS [107] found some sensitivity. When both ρ_{bb} and ρ_{tt} are nonzero, one may also have $gg \to b\bar{b}A/H \to b\bar{b}t\bar{t}$, which are covered in refs. [101–105].

3 Parameter space

Let us find the allowed parameter space for m_A, m_H and $m_{H^\pm}$. The parameters in eq. (2.1) are required to satisfy perturbativity, tree-level unitarity and vacuum stability conditions, for which we utilized the public tool 2HDMC [112]. We express the quartic couplings η_1, η_{3-6} in terms of m_h, m_H, $m_{H^\pm}$, m_A, μ_{22}, γ, and v as [95]

$$\eta_1 = \frac{m_h^2 s_\gamma^2 + m_H^2 c_\gamma^2}{v^2}, \tag{3.1}$$

$$\eta_3 = \frac{2(m_{H^\pm}^2 - \mu_{22}^2)}{v^2}, \tag{3.2}$$

$$\eta_4 = \frac{m_h^2 c_\gamma^2 + m_H^2 s_\gamma^2 - 2m_{H^\pm}^2 + m_A^2}{v^2}, \tag{3.3}$$

$$\eta_5 = \frac{m_H^2 s_\gamma^2 + m_h^2 c_\gamma^2 - m_A^2}{v^2}, \tag{3.4}$$

$$\eta_6 = \frac{(m_h^2 - m_H^2)(-s_\gamma)c_\gamma}{v^2}. \tag{3.5}$$

The quartic couplings η_2 and η_7 do not enter scalar masses, nor the mixing angle γ. Therefore in our analysis we take v, m_h, and γ, m_A, m_H, $m_{H^\pm}$, μ_{22}, η_2, η_7 as the phenomenological parameters. Further, to save computation time, we randomly generated these parameters in the following ranges: $\mu_{22} \in [0, 1000]$ GeV, $m_A \in [250, 600]$ GeV, $m_H \in [250, 600]$ GeV, $m_{H^\pm} \in [250, 600]$ GeV, $\eta_2 \in [0, 6]$, $\eta_7 \in [-6, 6]$, while satisfying

---

[4]Discussions on similar processes can also be found in refs. [97–100].

[5]For recent discussions see e.g. refs. [101–104].

[6]For a recent reference see also ref. [108].

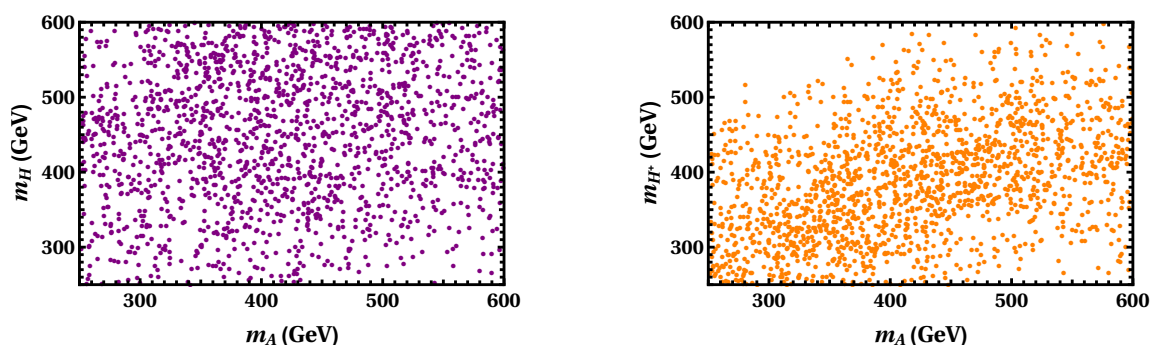[7]See e.g. for a non exhaustive list refs. [109–111].

Figure 1. Scanned points plotted in m_A–m_H (left) and m_A–$m_{H^\pm}$ (right) plane. Here the scanned points satisfy the tree level unitarity, perturbativity and positivity conditions as well as the T parameter constraint. However, not all points lead to the strong first-order EWPT.

$m_h = 125\,\text{GeV}$ with $c_\gamma = 0.1$.[8] The randomly generated parameters are then fed into 2HDMC for scanning. 2HDMC utilizes [112] $m_{H^\pm}$ and Λ_{1-7} as the input parameters in the Higgs basis whereas $v \simeq 246\,\text{GeV}$. In order to match the 2HDMC convention, we identify η_{1-7} as Λ_{1-7} and, take $-\pi/2 \leq \gamma \leq \pi/2$. For the positivity conditions of the Higgs potential of eq. (2.1), the parameter $\eta_2 > 0$ along with other more involved conditions implemented in 2HDMC. We further conservatively demand $|\eta_i| \leq 6$.

Next we impose the stringent oblique T parameter [113] constraint, which restricts hierarchical structures among the scalar masses m_H, m_A and $m_{H^\pm}$ [114, 115], and hence η_is. Utilizing the expression given in ref. [115] the points that passed unitarity, perturbativity and positivity conditions from 2HDMC, are further required to satisfy the T parameter constraint within the 2σ error [116].[9] These points are denoted as "scanned points". We plot the scanned points in the m_A–m_H and m_A–$m_{H^\pm}$ planes in the left and right panels of figure 1, which illustrates that significant amounts of the allowed points exists. A more detailed discussions on the scanning procedure can be found in refs. [118, 119]. At this point, we have not yet required that EWPT should be strongly first order, and not all points are compatible with the ρ_{bb} EWBG.

To find the constraints on ρ_{bb} and ρ_{tt} and, subsequently analyze the potential of future probes we choose three benchmark points (BPs) from the scanned points in figure 1, which are summarized in table 1. Here, we also demand that the chosen parameter sets give rise to the strong first-order EWPT. The BPa and BPb are chosen such that $m_A < 2m_t$. Since there is no suppression from $\mathcal{B}(A \to t\bar{t})$, such a choice would enhance the discovery potential of $bg \to bA \to bZh$ and $gg \to t\bar{t}A \to t\bar{t}b\bar{b}$. For the BP$c$, where $m_A > 2m_t$, the $bg \to bA \to bt\bar{t}$ process[10] can provide additional probes for the parameter space. Further, for all three BPs, A is assumed to be lighter than H and $H^\pm$ to forbid $A \to ZH$ and

---

[8]Note that, for successful ρ_{bb} induced EWBG, one requires non vanishing c_γ as discussed in ref. [85]. It was shown that for $c_\gamma \sim 0.1$, current data still allows $\text{Im}(\rho_{bb}) \sim 0.15$–$0.2$, while $|\text{Im}(\rho_{bb})| \gtrsim 0.058$ is sufficient to account for the observed BAU [85].

[9]The latest value of T parameter is obtained from ref. [117].

[10]Note that for BPa and BPb one may have $bg \to bH \to b\bar{b}t\bar{t}$, which can resemble similar final state topologies as in $bg \to bA \to bt\bar{t}$. This would be discussed in the section 4.2.

BP	η_1	η_2	η_3	η_4	η_5	η_6	η_7	$m_{H^\pm}$ (GeV)	m_A (GeV)	m_H (GeV)	$\frac{\mu_{22}^2}{v^2}$
a	0.282	2.034	4.053	-1.039	1.343	-0.243	1.231	391	285	405	0.5
b	0.289	1.959	4.064	-0.418	1.56	-0.316	-1.216	414	334	456	0.8
c	0.303	0.413	5.129	-0.477	1.534	-0.455	0.457	508	444	541	1.7

Table 1. Parameter values of three benchmark points chosen from the scanned points in figure 1, which are consistent with the strong first-order EWPT.
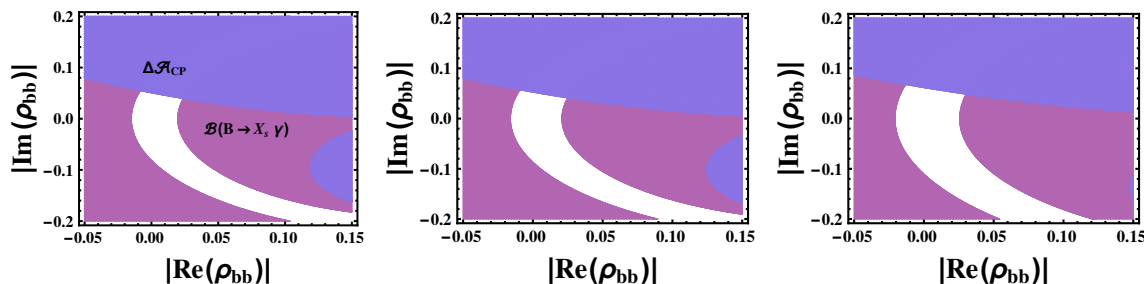

Figure 2. The constraints on ρ_{bb} from $\mathcal{B}(B \to X_s \gamma)$ (purple) and $\Delta\mathcal{A}_{CP}$ (blue) measurements for the BPa (left), BPb (middle) and BPb (right) respectively. All three figures are generated assuming $\rho_{tt} = 0.5$. See text for details.

$A \to H^\pm W^\mp$ decays and boost the discovery potential of these processes to some extent. Heavier A are indeed possible, but the cross sections are reduced due to rapid fall in the parton luminosity. We also remark that one requires [4–14] sub-TeV m_A, $m_{H^\pm}$ and m_H for the strong first-order EWPT, which is required for conventional sub-TeV EWBG [15–77] (for high-scale EWBG, see, e.g., refs. [87–89]).

In the following we will scrutinize the relevant constraints on ρ_{bb} and ρ_{tt}. For simplicity, we assume that ρ_{ij} except for ρ_{bb}, ρ_{tt} and ρ_{ee} are negligibly small so as not to affect our main discussion. The impacts of nonzero ρ_{ij} would be discussed later part of the paper.

3.1 Flavor constraints

There exist several constraints from flavor physics that restricts the parameter space. In particular, the following three observables are relevant: (i) the branching ratio measurement of $B \to X_s \gamma$ ($\mathcal{B}(B \to X_s \gamma)$), (ii) the asymmetry of the CP asymmetry between the charged and neutral $B \to X_s \gamma$ decays ($\Delta\mathcal{A}_{CP}$) and (iii) the B_q-$\overline{B}_q$ ($q = d, s$) mixings.

Let us first focus on $\mathcal{B}(B \to X_s \gamma)$. Non-zero ρ_{bb} and ρ_{tt} modify $\mathcal{B}(B \to X_s \gamma)$ via top quark and charged Higgs boson loop. The modification is parametrized by the (LO) Wilson coefficients $C_{7,8}^{(0)}$ at the matching scale $\mu = m_W$

$$C_{7,8}^{(0)}(m_W) = F_{7,8}^{(1)}(x_t) + \delta C_{7,8}^{(0)}(\mu_W), \tag{3.6}$$

where, $\overline{m}_t(m_W)$ is the top quark $\overline{\text{MS}}$ running mass at the m_W scale with $x_t = (\overline{m}_t(m_W)/m_W)^2$. The expression for $F_{7,8}^{(1)}(x)$ can be found in the refs. [120, 121], whereas

$\delta C_{7,8}^{(0)}(\mu_W)$ the LO (leading order) charged Higgs contributions. At LO, $\delta C_{7,8}^{(0)}(\mu_W)$ is expressed as [122]

$$\delta C_{7,8}^{(0)}(m_W) \simeq \frac{|\rho_{tt}|^2}{3\lambda_t^2} F_{7,8}^{(1)}(y_{H^+}) - \frac{\rho_{tt}\rho_{bb}}{\lambda_t\lambda_b} F_{7,8}^{(2)}(y_{H^+}), \tag{3.7}$$

with $y_{H^+} = (\overline{m}_t(m_W)/m_{H^+})^2$ while, the full expression for $F_{7,8}^{(2)}(y_{H^+})$ can be found in ref. [120]. The current world average of $\mathcal{B}(B \to X_s\gamma)_{\text{exp}}$ extrapolated to the photon-energy cut $E_0 = 1.6\,\text{GeV}$ is found by the HFLAV Collaboration to be $(3.32 \pm 0.15) \times 10^{-4}$ [123]. The next-to-next-to LO (NNLO) $\mathcal{B}(B \to X_s\gamma)$ prediction in the SM for the same photon-energy cut is $(3.36 \pm 0.23) \times 10^{-4}$ [124]. In order to find the constraint, we adopt the prescription outlined in ref. [125] and define

$$R_{\text{exp}} = \frac{\mathcal{B}(B \to X_s\gamma)_{\text{exp}}}{\mathcal{B}(B \to X_s\gamma)_{\text{SM}}}. \tag{3.8}$$

Based on our LO Wilson coefficients, we further express

$$R_{\text{theory}} = \frac{\mathcal{B}(B \to X_s\gamma)_{\text{g2HDM}}}{\mathcal{B}(B \to X_s\gamma)_{\text{SM}}}, \tag{3.9}$$

and take m_W and $\overline{m}_b(m_b)$ respectively as the matching scale and the low-energy scales. Finally, we demand R_{theory} to remain within the 2σ error of R_{exp}. In figure 2 the excluded regions are shown as the purple shaded regions in the $\text{Re}(\rho_{bb})$–$\text{Im}(\rho_{bb})$ plane for three BPs. Here, we assume $\rho_{tt} = 0.5$. Flavor constraints on ρ_{tt} is moderately strong, with $B_{d,s}$-$\overline{B}_{d,s}$ mixings providing the most stringent constraint on ρ_{tt} for $500 \lesssim m_{H^+} \lesssim 650\,\text{GeV}$, which is the ballpark mass ranges of $m_{H^\pm}$ for all the three BPs. The B_q-$\overline{B}_q$ mixing amplitude M_{12}^q receives modification from the charged Higgs and W bosons loop with t quark. Utilizing the expression for B_q-$\overline{B}_q$ mixing in type-II 2HDM [126], it is found in ref. [122] that

$$\frac{M_{12}^q}{M_{12}^{q\,\text{SM}}} = 1 + \frac{I_{WH}(y_W, y_H, x) + I_{HH}(y_H)}{I_{WW}(y_W)}, \tag{3.10}$$

where $y_i = m_t^2/m_i^2$ $(i = W, H^\pm)$ and $x = m_{H^\pm}^2/m_W^2$ with m_t and m_W being the masses of the top quark and W bosons. The expressions for I_{WW}, I_{WH} and I_{HH} are respectively given by [122]

$$I_{WW} = 1 + \frac{9}{1-y_W} - \frac{6}{(1-y_W)^2} - \frac{6}{y_W}\left(\frac{y_W}{1-y_W}\right)^3 \ln y_W, \tag{3.11}$$

$$I_{WH} \simeq \left(\frac{\rho_{tt}^*}{\lambda_t} + \frac{V_{cb}\rho_{ct}^*}{V_{tb}\lambda_t}\right)\left(\frac{\rho_{tt}}{\lambda_t} + \frac{V_{cq}^*\rho_{ct}}{V_{tq}^*\lambda_t}\right)y_H$$
$$\times \left[\frac{(2x-8)\ln y_H}{(1-x)(1-y_H)^2} + \frac{6x\ln y_W}{(1-x)(1-y_W)^2} - \frac{8-2y_W}{(1-y_W)(1-y_H)}\right], \tag{3.12}$$

$$I_{HH} \simeq \left(\frac{\rho_{tt}^*}{\lambda_t} + \frac{V_{cb}\rho_{ct}^*}{V_{tb}\lambda_t}\right)^2\left(\frac{\rho_{tt}}{\lambda_t} + \frac{V_{cq}^*\rho_{ct}}{V_{tq}^*\lambda_t}\right)^2\left(\frac{1+y_H}{(1-y_H)^2} + \frac{2y_H\ln y_H}{(1-y_H)^3}\right)y_H. \tag{3.13}$$

For $|\rho_{tt}| \sim \mathcal{O}(1)$ coupling ρ_{ct} is strongly constrained due to $|V_{cq}/V_{tq}| \sim 25$ ($q = d,\ s$) enhancement [122], as can be seen from eqs. (3.12) and (3.13). As we are primarily interested in the parameter space where ρ_{tt} is $\mathcal{O}(1)$, we turn off ρ_{ct} throughout our paper for

simplicity. The 2018 summer results of UTfit finds [127]:[11]

$$C_{B_d} \in 1.05 \pm 0.11,$$
$$C_{B_s} \in 1.110 \pm 0.090,$$
$$\phi_{B_d} \in -2.0 \pm 1.8 \text{ [in °]},$$
$$\phi_{B_s} \in 0.42 \pm 0.89 \text{ [in °]}. \tag{3.14}$$

with $M_{12}^q/M^{q \, \text{SM}} = C_{B_q} e^{2i\phi_{B_q}}$. Under the assumption on the ρ_{ij}^F couplings made in our analysis, we have $M_{12}^q/M^{q \, \text{SM}} = C_{B_q}$. Allowing 2σ errors on C_{B_d} and C_{B_s} we find that $B_{s,d}$-$\overline{B}_{d,s}$ mixings exclude $|\rho_{tt}| \gtrsim 0.9$ for BPa and BPb and, $|\rho_{tt}| \gtrsim 1$ for BPc.

One of the most powerful probes of $\text{Im}(\rho_{bb})$ is the direct CP asymmetry $\mathcal{A}_{\text{CP}}$ [129] of $B \to X_s \gamma$. It is advocated in ref. [130], however, that $\Delta\mathcal{A}_{\text{CP}}$ is even more sensitive to the CP-violating couplings, which is defined as [130]

$$\Delta\mathcal{A}_{\text{CP}} = \mathcal{A}_{B^- \to X_s^- \gamma} - \mathcal{A}_{B^0 \to X_s^0 \gamma} \approx 4\pi^2 \alpha_s \frac{\tilde{\Lambda}_{78}}{m_b} \text{Im}\left(\frac{C_8}{C_7}\right), \tag{3.15}$$

where $\tilde{\Lambda}_{78}$ and α_s denote a hadronic parameter and the strong coupling constant at $\overline{m}_b(m_b)$ scale, respectively. One expects that $\tilde{\Lambda}_{78}$ has a similar scale of Λ_{QCD}. In ref. [130], it is found that $17 \text{ MeV} \leq \tilde{\Lambda}_{78} \leq 190 \text{ MeV}$. On the other hand, recently Belle measured $\Delta\mathcal{A}_{\text{CP}} = (+3.69 \pm 2.65 \pm 0.76)\%$ [131], where the first uncertainty is statistical while the second one is systematic. Allowing 2σ error on the Belle measurement, we show the regions excluded by $\Delta\mathcal{A}_{\text{CP}}$ in blue shade in figures 2 for the three BPs. Here, we choose the average value of $\tilde{\Lambda}_{78}$ i.e., 89 MeV for illustration. We stress that the constraint shown in figures 2 depends heavily on the value of $\tilde{\Lambda}_{78}$. The larger $\tilde{\Lambda}_{78}$ would make the constraint stronger. We also remark that we utilize the LO Wilson coefficients in eq. (3.6) as a first approximation for simplicity. Note that the excluded regions by $\Delta\mathcal{A}_{\text{CP}}$ measurement in figure 2 is asymmetric and constrains positive $\text{Im}(\rho_{bb})$ more stringently. This is solely due to our choice of $\rho_{tt} = 0.5$. If we take $\rho_{tt} = -0.5$, the blue shaded regions would flip and exclude the negative regions of $\text{Im}(\rho_{bb})$.

We note in passing that if ρ_{tt} is also complex, $\Delta\mathcal{A}_{\text{CP}}$ can be zero if the complex phases of ρ_{tt} and ρ_{bb} are aligned, i.e., $\text{Im}(\rho_{tt}\rho_{bb})=0$, equivalently, $\text{Re}\rho_{bb}/\text{Re}\rho_{tt} = -\text{Im}\rho_{bb}/\text{Im}\rho_{tt}$. Such a phase alignment is discussed in ref. [86].

3.2 EDMs

The complex phase of ρ_{bb} is severely constrained by EDMs of the electron, neutron, and atoms, etc. Currently, the most stringent experimental bound comes from EDM of thorium monoxide (ThO), which is approximately given by

$$d_{\text{ThO}} = d_e + \alpha_{\text{ThO}} C_S, \tag{3.16}$$

where d_e is the electron EDM and C_S is the coefficient of the nuclear spin-independent interaction (NSID), which are respectively defined as

$$\mathcal{L}_{\text{EDM}} = -\frac{i}{2} d_e F^{\mu\nu} \bar{e} \sigma_{\mu\nu} \gamma_5 e, \quad \mathcal{L}_{eN}^{\text{NSID}} = -\frac{G_F}{\sqrt{2}} C_S (\bar{N}N)(\bar{e}i\gamma_5 e), \tag{3.17}$$

---

[11]The New Physics Fit results of 2018 Summer can be found at ref. [128].
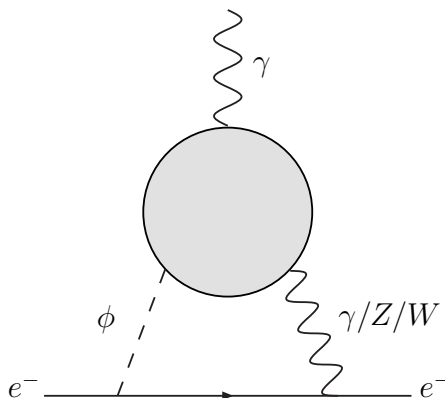
Figure 3. Two-loop Barr-Zee diagrams contributing to the electron EDM, where $\phi = h, H, A, H^{\pm}$. The shaded loop collectively represents the scalar, fermion and gauge boson loops. The total contribution is given by their sum, $d_e = d_e^{\phi\gamma} + d_e^{\phi Z} + d_e^{\phi W}$.

where $F^{\mu\nu}$ denotes the field strength tensor of electromagnetism and G_F is the Fermi coupling constant. The coefficient α_{ThO} is estimated as $\alpha_{\mathrm{ThO}} = 1.5 \times 10^{-20}$ [132]. The latest experimental value of d_{ThO} is placed by ACME Collaboration in 2018 (ACME18) as

$$d_{\mathrm{ThO}} = (4.3 \pm 4.0) \times 10^{-30} \ e \ \mathrm{cm}, \tag{3.18}$$

from which under the assumption of $C_S = 0$ the electron EDM has an upper bound of

$$|d_e| < 1.1 \times 10^{-29} \ e \ \mathrm{cm}. \tag{3.19}$$

In our scenario, d_e is predominantly induced by two-loop Barr-Zee diagrams as depicted in figure 3, which are decomposed into the three parts:

$$d_e = d_e^{\phi\gamma} + d_e^{\phi Z} + d_e^{\phi W}, \tag{3.20}$$

where $\phi = h, H, A$ for the first two terms and $\phi = H^{\pm}$ for the last term. Let us denote the contribution of i-species to $d_e^{\phi\gamma}$ as $(d_e^{\phi\gamma})_i$. If ρ_{bb} is the only source of CP violation, $d_e \simeq (d_e^{\phi\gamma})_b$. With $\mathrm{Im}\rho_{bb}$ required by ρ_{bb}-EWBG mechanism, d_e is so large that one cannot avoid the ACME18 bound as noted in ref. [85]. This fact suggests two options: (i) the alignment limit ($c_\gamma \to 0$) and (ii) cancellation mechanism. As discussed in ref. [86], however, the first option may not be consistent with EWBG in g2HDM since the BAU would be suppressed with decreasing c_γ. We thus consider the second option. Even though we identify the parameter space for the cancellation in ref. [85], we do not show its detail there, and moreover, $d_e^{\phi W}$, which can come into play in the cancellation region, is missing. We therefore update our previous analysis taking all the relevant contributions into consideration.

If there exist more than two CP-violating phases, we could tune the parameters in such a way that d_e becomes small. While it is nothing more than the parameter turning, we still classify the cancellation parameter space into two kind. We call a cancellation *structured cancellation* if it happens when the hierarchical structures of the ρ_{ij} matrices

closely resemble those of the SM Yukawa matrices, and anything else is *unstructured cancellation*. It is revealed in ref. [86] that the parameter space of ρ_{tt}-EWBG accommodates the structured cancellation. We here scrutinize the type of the cancellation in ρ_{bb}-EWBG.

Following a method adopted in ref. [86], we split $(d_e^{\phi\gamma})_b$ into two parts as[12]

$$(d_e^{\phi\gamma})_f = (d_e^{\phi\gamma})_f^{\text{mix}} + (d_e^{\phi\gamma})_f^{\text{extr}}, \tag{3.21}$$

where

$$\frac{(d_e^{\phi\gamma})_f^{\text{mix}}}{e} = -\frac{3\alpha_{\text{em}}Q_f^2 s_{2\gamma}}{16\sqrt{2}\pi^3 v}\left[\text{Im}(\rho_{ee})\Delta f_f + \frac{\lambda_e}{\lambda_f}\text{Im}(\rho_{ff})\Delta g_f\right], \tag{3.22}$$

$$\frac{(d_e^{\phi\gamma})_f^{\text{extr}}}{e} = \frac{3\alpha_{\text{em}}Q_f^2}{16\pi^3 m_f}\left[\text{Im}(\rho_{ee})\text{Re}(\rho_{ff})\left\{c_\gamma^2 f(\tau_{fh}) + s_\gamma^2 f(\tau_{fH}) \pm g(\tau_{fA})\right\}\right.$$
$$\left. + \text{Im}(\rho_{ff})\text{Re}(\rho_{ee})\left\{c_\gamma^2 g(\tau_{fh}) + s_\gamma^2 g(\tau_{fH}) \pm f(\tau_{fA})\right\}\right], \tag{3.23}$$

with α_{em} and Q_f representing the fine structure constant and electric charges of f, respectively, and $\Delta f_f = f(\tau_{fh}) - f(\tau_{fH})$ and $\Delta g_f = g(\tau_{fh}) - g(\tau_{fH})$ with $\tau_{ij} = m_i^2/m_j^2$. $f(\tau)$ and $g(\tau)$ are the loop functions and their explicit forms are shown in appendix A. In our notation, the sign of e is positive. In the wave parenthesis in eq. (3.23), the upper sign is for up-type fermions and the lower is for down-type fermions, respectively. For $c_\gamma \ll 1$ and $m_H \simeq m_A$, $(d_e^{\phi\gamma})_{t,b}^{\text{extr}}$ are approximated as

$$\frac{(d_e^{H\gamma})_t^{\text{extr}}}{e} \simeq \frac{\alpha_{\text{em}}}{12\pi^3 m_t}\text{Im}(\rho_{ee}\rho_{tt})\left[f(\tau_{tH}) + g(\tau_{tH})\right], \tag{3.24}$$

$$\frac{(d_e^{H\gamma})_b^{\text{extr}}}{e} \simeq \frac{\alpha_{\text{em}}}{48\pi^3 m_b}\text{Im}(\rho_{ee}\rho_{bb}^*)\left[f(\tau_{bH}) - g(\tau_{bH})\right]. \tag{3.25}$$

In the ρ_{bb}-EWBG scenario, $\text{Im}(\rho_{ee}\rho_{tt}) = \rho_{tt}\text{Im}(\rho_{ee})$. To make our discussion on the cancellation mechanism simpler, we consider a case in which $\text{Im}(\rho_{ee}\rho_{bb}^*) \simeq 0$ so that $(d_e^{\phi\gamma})_b \simeq (d_e^{\phi\gamma})_b^{\text{mix}}$. When ρ_{ee} is nonzero, the primary contribution could be $(d_e^{\phi\gamma})_W$ as inferred from the fact that the ϕ-γ-γ vertex in $d_e^{\phi\gamma}$ is more or less common to the $h \to 2\gamma$ decay. Noting that the W-loop has only the "mix" contribution since the Higgs couplings to the W bosons are the gauge couplings, one may find [133]

$$\frac{(d_e^{H\gamma})_W}{e} = \frac{(d_e^{H\gamma})_W^{\text{mix}}}{e} = \frac{\alpha_{\text{em}}s_{2\gamma}}{64\sqrt{2}\pi^3 v}\text{Im}(\rho_{ee})\Delta\mathcal{J}_W^\gamma, \tag{3.26}$$

where $\Delta\mathcal{J}_W^\gamma = \mathcal{J}_W^\gamma(m_h) - \mathcal{J}_W^\gamma(m_H)$ (for explicit form of $\mathcal{J}_W^\gamma$, see appendix A). From the condition of $(d_e^{\phi\gamma})_t + (d_e^{\phi\gamma})_b + (d_e^{\phi\gamma})_W = 0$, it follows that

$$\frac{\text{Im}(\rho_{ee})}{\text{Im}(\rho_{bb})} = -\frac{s_{2\gamma}\Delta g_b/4}{s_{2\gamma}[\Delta f_t + \Delta f_b/4 - (3/16)\Delta\mathcal{J}_W^\gamma] + 2\rho_{tt}[f(\tau_{tH}) + g(\tau_{tH})]/\lambda_t} \equiv -c \times \frac{\lambda_e}{\lambda_b}. \tag{3.27}$$

It is found that $c = 1.0 \times 10^{-3}$ for $c_\gamma = 0.1$, $\rho_{tt} = 0.5$, $m_h = 125\,\text{GeV}$ and $m_H = 405\,\text{GeV}$. Therefore, the cancellation is possible but unstructured since c deviates much from the unity

---

[12]By convention in this paper, the sign of γ is opposite to that in ref. [86].

as opposed to the ρ_{tt}-EWBG scenario [86]. Once this accidental cancellation happens, other contributions could become relevant. On the grounds of dimensional analysis, one can find that $d_e^{\phi Z}$ is suppressed by the Z boson coupling to the electron, $g_{Zee} = 1/4 - \sin\theta_W \simeq 0.02$ with θ_W representing the weak mixing angle, while $d_e^{\phi W}$ is not and becomes leading contribution. The dominant contribution in $d_e^{\phi W}$ comes from the diagrams involving the top and bottom loops, which amounts to [86, 134, 135]

$$\frac{(d_e^{\phi W})_{t/b}}{e} \simeq \frac{3\alpha_{\mathrm{em}}|V_{tb}|^2}{128\pi^3 s_W^2} \frac{m_t}{m_{H^\pm}^2} \mathrm{Im}(\rho_{ee}\rho_{tt}) J_1(\tau_{WH^\pm}, \tau_{tH^\pm}), \tag{3.28}$$

where $m_b = 0$ and V_{tb} is the (33) element of the CKM matrix, which is close to one [1]. J_1 is the loop function listed in appendix A. In general, this contribution has the ρ_{bb} dependence but vanishes in the case of $m_b = 0$. Note that $(d_e^{\phi W})_{t/b}$ is absent in the softly-broken Z_2 2HDMs. For one of the ρ_{bb}-EWBG parameter points, e.g., $\mathrm{Im}(\rho_{bb}) = -0.15$, one would get $(d_e^{\phi W})_{t/b} \simeq 1.2 \times 10^{-29}\, e$ cm in the cancellation region specified by eq. (3.27), together with $m_{H^\pm} = 391\,\mathrm{GeV}$ and $\rho_{tt} = 0.5$, which slightly exceeds the ACME18 bound. Therefore, the allowed region is not exactly determined by the cancellation condition but it occurs in its vicinity, as we show in our numerical analysis conducted below. It should be noted that even though ρ_{tt} is real in ρ_{bb}-EWBG, its magnitude can be constrained by the electron EDM due to the proportionality of $\rho_{tt}\mathrm{Im}(\rho_{ee})$.

Now we move on to discuss the C_S contribution. We estimate C_S using the CP-violating 4-fermion interactions between the quarks and electron defined as

$$\mathcal{L}_{4f}^{\mathrm{CPV}} = \sum_q C_{qe}(\bar{q}q)(\bar{e}i\gamma_5 e), \tag{3.29}$$

where $C_{qe} = \sum_{\phi=h,H,A} g_{\phi\bar{q}q}^S g_{\phi\bar{e}e}^P / m_\phi^2$ (explicit forms of $g_{\phi\bar{q}q}^S$ and $g_{\phi\bar{e}e}^P$ are shown in appendix A) With those, C_S is estimated as [136]

$$C_S = -2v^2 \left[6.3(C_{ue} + C_{de}) + C_{se}\frac{41\ \mathrm{MeV}}{m_s} + C_{ce}\frac{79\ \mathrm{MeV}}{m_c} + 62\ \mathrm{MeV}\left(\frac{C_{be}}{m_b} + \frac{C_{te}}{m_t}\right) \right]. \tag{3.30}$$

Note that for $c_\gamma \ll 1$ and $m_H \simeq m_A$, C_{qe} for up- and down-type quarks are, respectively, cast into the form [86]

$$C_{ue} \simeq \frac{1}{2m_H^2}\mathrm{Im}(\rho_{ee}\rho_{uu}), \quad C_{de} \simeq \frac{1}{2m_H^2}\mathrm{Im}(\rho_{ee}\rho_{dd}^*). \tag{3.31}$$

Therefore, the dependences of the CP-violating phases are the same as those of $(d_e^{\phi\gamma})_u^{\mathrm{extr}}$ and $(d_e^{\phi\gamma})_d^{\mathrm{extr}}$, respectively.

In our numerical analysis, we parametrize ρ_{ff}, except for ρ_{tt}, as $\mathrm{Re}(\rho_{ee}) = -r(\lambda_e/\lambda_b)\mathrm{Re}(\rho_{bb})$ and $\mathrm{Im}(\rho_{ee}) = -r(\lambda_e/\lambda_b)\mathrm{Im}(\rho_{bb})$. Though the CP-violating phases in the first and second generations of ρ^F matrices have nothing to do with ρ_{bb}-EWBG, we fix them through the above relations. However, the effects of the extra CP violation are too small to affect our cancellation mechanism in ρ_{bb}-EWBG.

In figure 4, $|d_{\mathrm{ThO}}|$ and its details are shown as functions of r. We take BPa for the Higgs spectrum and set $c_\gamma = 0.1$, $\mathrm{Re}(\rho_{bb}) = 0$, $\mathrm{Im}(\rho_{bb}) = -0.15$ and $\rho_{tt} = 0.5$ as an example
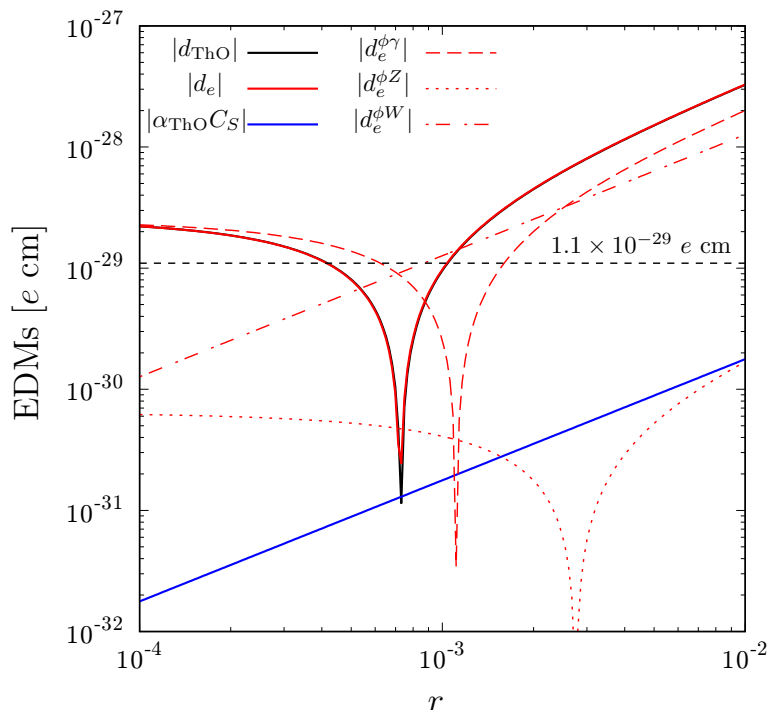
Figure 4. Details of EDMs as functions of r. We take BPa for the Higgs spectrum and set $c_\gamma = 0.1$, $\mathrm{Re}(\rho_{bb}) = 0$, $\mathrm{Im}(\rho_{bb}) = -0.15$ and $\rho_{tt} = 0.5$ as an example of the ρ_{bb}-EWBG scenario. Other ρ_{ff} are fixed by $\mathrm{Re}(\rho_{ee}) = -r(\lambda_e/\lambda_b)\mathrm{Re}(\rho_{bb})$ and $\mathrm{Im}(\rho_{ee}) = -r(\lambda_e/\lambda_b)\mathrm{Im}(\rho_{bb})$. The ACME18 bound ($|d_e| < 1.1 \times 10^{-29}$ e cm) is shown by the horizontal dotted line in black.

of the ρ_{bb}-EWBG scenario. As seen, the magnitude of $\alpha_{\mathrm{ThO}}C_S$ is much smaller than that of d_e, we thus can use the ACME18 bound of $|d_e| < 1.1 \times 10^{-29}$ e cm, which is represented by the horizontal dotted line in black, to constrain the parameter space. As discussed in eq. (3.27), the cancellation happens in $d_e^{\phi\gamma}$ at around $r \simeq 1 \times 10^{-3}$, which is the consequences of $(d_e^{\phi\gamma})_t + (d_e^{\phi\gamma})_b + (d_e^{\phi\gamma})_W \simeq 0$. At this point, $d_e^{\phi W}$ becomes dominant and $|d_e|$ exceeds the ACME 18 bound. Nevertheless, the cancellation is still at work at around $r \simeq 0.7 \times 10^{-3}$. Similar to this case, we can always find cancellation regions in the cases of BPb and BPc as well, and thus conclude that ρ_{bb}-EWBG scenario is still consistent with the ACME18 bound. Note that here we set $c_\gamma = 0.1$ while finding the constraints from ACME18 to illustrate $\mathrm{Im}(\rho_{bb}) \sim 0.15$ is still allowed for $\rho_{tt} \sim 0.5$ for all the three BPs. In the rest of the paper, however, we ignore the c_γ dependence since it is insensitive to our collider study.

Here, we briefly discuss the EDMs of neutron and Mercury. Their current experimental values are respectively given by [137, 138]

$$|d_n| < 1.8 \times 10^{-26} \ e \ \mathrm{cm} \ (90\% \ \mathrm{C.L.}), \tag{3.32}$$

$$|d_{\mathrm{Hg}}| < 7.4 \times 10^{-30} \ e \ \mathrm{cm} \ (95\% \ \mathrm{C.L.}). \tag{3.33}$$

On the theoretical side, the neutron EDM based on QCD sum rules is estimated as [139],

$$d_n = -0.20 d_u + 0.78 d_d + e(0.29 d_u^C + 0.59 d_d^C)/g_3, \tag{3.34}$$

where g_3 is the $\mathrm{SU}(3)_C$ gauge coupling and d_q^C are the quark chromo EDMs defined by the operator $\mathcal{L}_{\mathrm{CEDM}} = -(i/2)d_q^C G^{\mu\nu} \bar{q}\sigma_{\mu\nu}\gamma_5 q$ with $G^{\mu\nu}$ representing $\mathrm{SU}(3)_C$ field strength tensor. We note that even though the cancellation mechanism can work in d_n as well, it does not occur at the cancellation point of d_e. Using the same input parameters as in figure 4 with $r = 0.7 \times 10^{-3}$, we obtain $|d_n| = 2.4 \times 10^{-29}$ e cm, which is nearly 3 orders of magnitude below the current bound. For the mercury EDM, on the other hand, we estimate it using formulas in refs. [140–142] assuming $d_{\mathrm{Hg}}^{\mathrm{I}}$ defined in ref. [141] and find that $|d_{\mathrm{Hg}}| = 8.0 \times 10^{-31}$ e cm, which is smaller than the current bound by about 1 order of magnitude.

We note in passing that a future measurement of the proton EDM could be another good prober of ρ_{bb}-EWBG. The experimental sensitivity of the proton EDM at IBS-CAPP [143] and BNL [144] is $|d_p| \sim 10^{-29}$ e cm. As is the case of neutron EDM discussed above, the proton EDM can be estimated by use of the QCD sum rules as [139]

$$d_p = 0.78 d_u - 0.20 d_d + e(-1.2 d_u^C - 0.15 d_d^C)/g_3. \tag{3.35}$$

With this, it is found that $|d_p| = 6.1 \times 10^{-29}$ e cm for the parameters used in figure 4 with $r = 0.7 \times 10^{-3}$. Therefore, the future measurement of d_p could access the ρ_{bb}-EWBG parameter space regardless of the d_e cancellation.

3.3 Direct search limits

There exist several direct search limits from ATLAS and CMS that may restrict the parameter space of ρ_{bb}, even for $c_\gamma = 0$ and $\rho_{tt} = 0$. The coupling ρ_{bb} receives several constraints from heavy Higgs boson searches at the LHC. In particular, refs. [145–149] are relevant to our study. We find that the most stringent constraint arises from CMS search involving heavy Higgs boson production in association with at least one b-jet and decaying into $b\bar{b}$ pair based on 13 TeV 35.7 fb^{-1} data [145]. The CMS search provides a model independent 95% CL upper limits on the $\sigma(pp \to bA/H + X) \cdot \mathcal{B}(A/H \to b\bar{b})$ in the mass range beginning from 300 GeV to 1300 GeV. We first extract[13] corresponding 95% CL upper limit $\sigma(pp \to bA/H + X) \cdot \mathcal{B}(A/H \to b\bar{b})$ for our three BPs. Taking a reference $|\rho_{bb}|$ value, we then estimate the production cross sections of $pp \to bA/H + X$ at the leading order (LO) utilizing Monte Carlo event generator MadGraph5_aMC@NLO [150] (denoted as Mad-Graph5_aMC) with the default parton distribution function (PDF) NN23LO1 set [151] for the BPs. As the analysis does not veto additional activity in the event [145], we therefore include contributions from $gg \to b\bar{b}A/H$ along with $bg \to bA/H$ while estimating the cross sections. These cross sections are finally rescaled by $|\rho_{bb}|^2 \times \mathcal{B}(A/H \to b\bar{b})$, assuming $\mathcal{B}(A/H \to b\bar{b}) = 100\%$, to obtain the corresponding 95% CL upper limits on $|\rho_{bb}|$. It is found that $|\rho_{bb}| \gtrsim 0.6$ is excluded for BPa at 95% CL and likewise, the regions where $|\rho_{bb}| \gtrsim 0.7$ are ruled out for both BPb and BPc. These upper limits are rather weak and would be further weakened by $\mathcal{B}(A \to Zh)$ and $\mathcal{B}(A/H \to t\bar{t})$. The limits are even weaker from a similar search performed by ATLAS [146]. We note that while estimating the upper limit

---

[13]To obtain the 95% CL $\sigma(pp \to bA/H + X) \cdot \mathcal{B}(A/H \to b\bar{b})$ upper limit for the three benchmark points BPI, BPII and BPIII, we digitized the figure of ref. [145]. The figure is available in http://cms-results.web.cern.ch/cms-results/public-results/publications/HIG-16-018/ along with other auxiliary materials (a similar digitization strategy was followed in ref. [177]).

on ρ_{bb} we set all $\rho_{ij} = 0$ for simplicity. In general, we remark that nonzero ρ_{ij} would further alleviate these upper limits. Further, ρ_{bb} coupling can induce $pp \to t(b)H^{\pm}$ process which is proportional to V_{tb} (see eq. (2.7)). These processes are extensively searched by ATLAS [147] and CMS [148, 149] with $H^+/H^- \to t\bar{b}/\bar{t}b$ decays. We find that the constraints are weaker for all the three BPs, however, as we see below these searches would provide sensitive probe to ρ_{tt}. The effective model is implemented in the FeynRules 2.0 [152] framework.

We now turn to constraints on ρ_{tt}. As ρ_{tt} can also induce V_{tb}, the searches $pp \to \bar{t}(b)H^+$ followed by $H^+ \to t\bar{b}$ [147–149] would also be relevant. The ATLAS search [147] is based on $36\,\mathrm{fb}^{-1}$ $\sqrt{s} = 13\,\mathrm{TeV}$ dataset, which provides model independent 95% CL upper limit on $\sigma(pp \to \bar{t}bH^+) \times \mathcal{B}(H^+ \to t\bar{b})$ from $m_{H^{\pm}} = 200\,\mathrm{GeV}$ and $2\,\mathrm{TeV}$. Similar searches are also performed by CMS based on $\sqrt{s} = 13\,\mathrm{TeV}$ $35.9\,\mathrm{fb}^{-1}$ dataset [148, 149]. These searches provide 95% CL upper limit on $\sigma(pp \to \bar{t}H^+) \times \mathcal{B}(H^+ \to t\bar{b})$ for $m_{H^{\pm}} = 200\,\mathrm{GeV}$ and $3\,\mathrm{TeV}$ in leptonic [148] and, combining leptonic and all-hadronic final states [149]. Like before, the nonvanishing ρ_{tt} enhanced by V_{tb} can induce such process, leading to stringent constraints. To find the constraints, as done before, we calculate the cross sections $\sigma(pp \to \bar{t}bH^+) \times (H^+ \to t\bar{b})$ at LO for a reference $|\rho_{tt}|$ for the three BPs via MadGraph5_aMC. These cross sections are then rescaled by $|\rho_{tt}|^2 \times \mathcal{B}(H^+ \to t\bar{b})$ to get the corresponding 95% CL upper limits on $|\rho_{tt}|$. The extracted (footnote 13) 95% CL upper limits from ATLAS search [147] on ρ_{tt} for the three BPs are $|\rho_{tt}| \gtrsim 0.7$, 0.8 and 1, respectively, while the limits from CMS [149] are much stronger, which read as $|\rho_{tt}| \gtrsim 0.6$, 0.61 and 0.61, respectively. We remark that the constraints from CMS search with leptonic final state [148] is mildly weaker than the search with combined leptonic and all-hadronic final states [149]. We also note that all the ρ_{ij} except for ρ_{tt} are assumed to be zero when extracting the upper limits for the sake of simplicity. Therefore if other ρ_{ij} are turned on, the limits on ρ_{tt} in general becomes weaker due to dilution from other branching ratios of $H^{\pm}$.

The ATLAS [106] and CMS [107] search for heavy Higgs via $gg \to H/A \to t\bar{t}$ would also constrain ρ_{tt}. The ATLAS [106] result is based on $20.3\,\mathrm{fb}^{-1}$ data at $8\,\mathrm{TeV}$, which provides exclusion limits on $\tan\beta$ vs m_A (or, m_H) in type-II 2HDM framework starting from m_A and $m_H = 500\,\mathrm{GeV}$. The CMS search is based on $35.9\,\mathrm{fb}^{-1}$ data at $\sqrt{s} = 13\,\mathrm{TeV}$, which provides upper limit on coupling modifier (see ref. [107] for definition) the m_A (m_H) from $400\,\mathrm{GeV}$ to $750\,\mathrm{GeV}$ based on different values of Γ_A/m_A (Γ_H/m_H) ratios. Given the values of m_A and m_H of the BPs, ATLAS search can only constrain BPc via $gg \to H \to t\bar{t}$. Reinterpreting the ATLAS exclusion limit [106], we find that $|\rho_{tt}| \gtrsim 0.8$ is excluded for BPc at 95% CL. On the other hand, for CMS search [107], $gg \to A \to t\bar{t}$ can constrain $|\rho_{tt}|$ only for BPc, whereas $gg \to H \to t\bar{t}$ constrains all three BPs. We find that CMS $gg \to A \to t\bar{t}$ search excludes the region of $|\rho_{tt}| \gtrsim 1$ (1.1) at 95% CL for BPc if $\Gamma_A/m_A = 5\%$ ($\Gamma_A/m_A = 10\%$). The $gg \to H \to t\bar{t}$ search places the constraints that $|\rho_{tt}| \gtrsim 1.6$ (2.1), 1.2 (1.4) and 1.2 (1.3) if $\Gamma_H/m_H = 5\%$ ($\Gamma_H/m_H = 10\%$) at 95% CL for the three BPs respectively. We remark that these upper limits provided by both the collaborations assume that m_A and m_H are decoupled from each other. Although m_A and m_H are separated sufficiently, this is not the case for any of the BPs chosen, as can be seen from table 1. Therefore, the actual upper limits extracted here would be mildly stronger.

BP	$\mathcal{B}(A \to b\bar{b})$	$\mathcal{B}(A \to Zh)$	$\mathcal{B}(A \to t\bar{t})$
a	0.95	0.05	—
b	0.89	0.11	—
c	0.12	0.04	0.84

Table 2. Branching ratios of A for the benchmark points in table 1 with $\mathrm{Re}(\rho_{bb}) = 0.0$, $|\mathrm{Im}(\rho_{bb})| = 0.15$ and $|\rho_{tt}| = 0.5$.

Moreover, ρ_{tt} would also receive constraint from CMS search for SM four-top production [153]. The search is performed with 13 TeV 137 fb^{-1} dataset and provides 95% CL upper limits on $\sigma(pp \to t\bar{t}A/t\bar{t}H) \times \mathcal{B}(A/H \to t\bar{t})$ for 350 GeV $\leq m_{A/H} \leq$ 650 GeV. The search also includes contributions from $\sigma(pp \to tWA/H, tqA/H)$ followed by $A/H \to t\bar{t}$, which can also be induced by ρ_{tt}. To understand how strong the constraints could be, we generate these cross sections at LO by MadGraph5_aMC for a reference value of $|\rho_{tt}|$ setting all other $\rho_{ij} = 0$, and then rescale simply by $|\rho_{tt}|^2 \times \mathcal{B}(A/H \to t\bar{t})$. Again, given the masses of BPs, the $\sigma(pp \to t\bar{t}A) \times \mathcal{B}(A \to t\bar{t})$ search can constrain only BPc, for which $|\rho_{tt}| \gtrsim 0.8$ excluded at 95% CL. However, $\sigma(pp \to t\bar{t}H) \times \mathcal{B}(H \to t\bar{t})$ can constrain all three BPs, and we find that the regions of $|\rho_{tt}| \gtrsim 0.9$, 0.8 and 1 are excluded at 95% CL, respectively, where $\mathcal{B}(A/H \to t\bar{t}) = 100\%$ is assumed. However, it should be noted that the presence of $\mathcal{B}(A/H \to b\bar{b})$ and $\mathcal{B}(A \to Zh)$ would alleviate the limits. As in the case of $gg \to H/A \to t\bar{t}$, the search here also assumes that m_A and m_H are decoupled from each other. Therefore, one expects the limits to be mildly stronger for all the three BPs.

We finally conclude that for $\mathrm{Re}(\rho_{bb}) \sim 0$, $c_\gamma = 0.1$, $|\mathrm{Im}(\rho_{bb})| \sim 0.15$ and $\rho_{tt} \sim 0.5$ are well allowed by the current measurements for the mass spectrum under consideration. We take these values as representative values for our analysis with $\mathrm{Re}(\rho_{bb}) = 0$.[14] Under the assumptions, i.e., setting all $\rho_{ij} = 0$ except ρ_{bb} and ρ_{tt}, the total decay width of A can be nicely approximated as the sum of the partial widths of $A \to b\bar{b}$ and $A \to Zh$ for BPa and BPb and, $A \to b\bar{b}$, $A \to Zh$ and $A \to t\bar{t}$ for BPc. The total decay widths of A are 0.4 GeV, 0.5 GeV and 4.97 GeV respectively for the three BPs with $|\mathrm{Im}(\rho_{bb})| \sim 0.15$ and $\rho_{tt} \sim 0.5$. The corresponding branching ratios are presented in table 2. Note that when calculating decay widths and branching ratios of A, we neglect tiny loop induced decays such as $A \to \gamma\gamma$, $A \to Z\gamma$ etc.

4 Collider signatures

4.1 The $bg \to bA \to bZh$ process

In this subsection we study the discovery potential of $bg \to bA \to bZh$ process at 14 TeV LHC. The process can be searched via $pp \to bA + X \to bZh + X$ followed by $Z \to \ell^+\ell^-$ ($\ell = e, \mu$) and $h \to b\bar{b}$, comprising three b-jets, same flavor opposite sign lepton pair (denoted

---

[14]As discussed before, both ρ_{bb} and ρ_{tt} can induce $pp \to t(b)H^\pm$ process, hence, the constraints from ref. [149] would become stronger if both the couplings are nonvanishing. However, we have checked that $\rho_{tt} \sim 0.5$ is allowed for $|\mathrm{Im}(\rho_{bb})| \sim 0.15$ for all the three BPs.
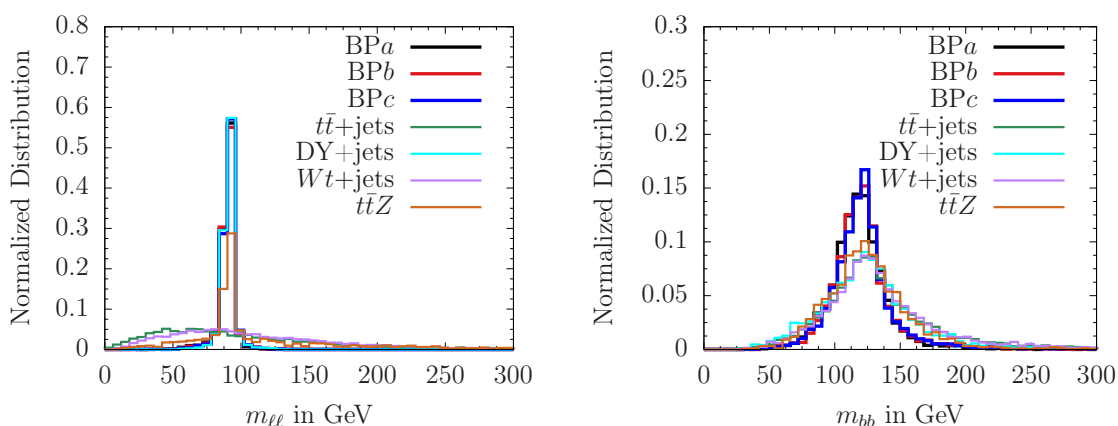
Figure 5. The normalized $m_{\ell\ell}$ (left) and m_{bb} (right) distributions of the three BPs and leading backgrounds for the bZh process.

as the bZh process). There are several SM backgrounds for this final state topology. The dominant backgrounds are $t\bar{t}$+jets, Drell-Yan+jets (DY+jets), Wt+jets, $t\bar{t}Z$+jets, $t\bar{t}h$, tZ+jets, with subdominant contributions arise from four-top ($4t$), $t\bar{t}W$, tWh, tWZ and WZ+jets. Backgrounds from WW+jets and ZZ+jets are negligibly small and hence not included. Note that one can also search for $h \to \gamma\gamma$ or $h \to \tau\tau$; however, we do not find them as promising.

The signal and background event samples are generated in pp collision with $\sqrt{s} = 14\,\text{TeV}$ CM energy at LO by MadGraph5_aMC with NN23LO1 PDF set as done before and then interfaced with Pythia 6.4 [154] for hadronization and showering and finally fed into Delphes 3.4.2 [155] for fast detector simulation adopting default ATLAS-based detector card. We adopt MLM scheme [156, 157] for matrix element and parton shower merging. Note that we have not included backgrounds from the fake and non-prompt sources in our analysis. Such backgrounds are not properly modeled in Monte Carlo simulations and requires data to estimate such contributions.

The LO $t\bar{t}$+jets and Wt+jets cross sections are normalized to NNLO (next-to-next-to LO) with NNLL (next-to-next-to leading logarithmic) corrections by factors 1.84 [158] and 1.35 [159] respectively. We normalize the DY+jets background cross section to the NNLO QCD+NLO EW one by factor 1.27, which is obtained by utilizing FEWZ 3.1 [160, 161]. The LO $t\bar{t}Z$, $\bar{t}Z+$ jets, $t\bar{t}h$, $4t$ and $t\bar{t}W^-$ ($t\bar{t}W^+$) cross sections are adjusted to NLO ones by K-factors 1.56 [162], 1.44 [150], 1.27 [163], 2.04 [150] and 1.35 (1.27) [164] respectively, but tWZ and tWh both are kept at LO. Finally, the background W^-Z+jets is normalized to NNLO by factor 2.07 [165]. For simplicity we assume the same QCD correction factors for the conjugate processes tZj and W^+Z+jets, while the signal cross sections are kept at LO.

To reduce backgrounds, we adopt following event selection criteria: each event should contain a same flavor opposite sign lepton pair and at least three b-tagged jets. The transverse momenta (p_T) of the leading and subleading leptons should be $> 28\,\text{GeV}$ and $> 25\,\text{GeV}$ respectively, whereas p_T for all three b-jets should be $> 20\,\text{GeV}$. The pseudorapidity ($|\eta|$) of the leptons and all three b-jets are required to be < 2.5. The jets are
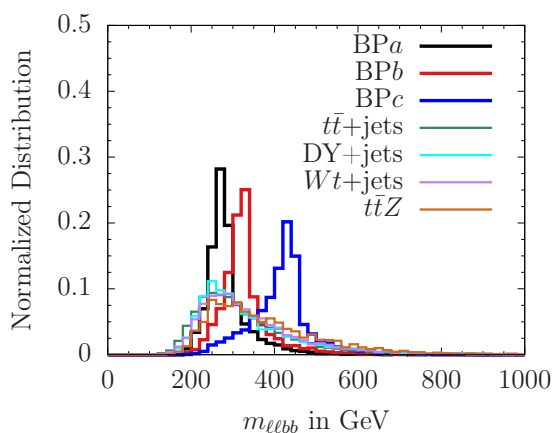
Figure 6. The normalized $m_{\ell\ell bb}$ distributions of the signal and leading backgrounds for the bZh process.

BP	$t\bar{t}+$ jets	$DY+$ jets	$Wt+$ jets	$t\bar{t}Z$	$t\bar{t}h$	$tZ+$ jets	Others	Total Bkg. (fb)
a	0.178	0.533	0.226	0.023	0.008	0.007	0.003	0.978
b	0.087	0.272	0.084	0.018	0.003	0.006	0.001	0.471
c	0.016	0.094	0.022	0.008	0.0002	0.002	0.0004	0.143

Table 3. The background cross sections (in fb) for the bZh process after selection cuts at $\sqrt{s} = 14\,$TeV LHC. Here we added together subdominant backgrounds $4t$, $t\bar{t}W$, tWh, tWZ and $WZ+$jets as "Others". The total background (Total Bkg.) yield is provided in last column.

BP	Signal (fb)	Significance ($\mathcal{Z}$) 300 (1000) fb^{-1}
a	0.17	2.9 (5.3)
b	0.228	5.4 (9.8)
c	0.027	1.2 (2.2)

Table 4. The signal cross sections after selection cuts and the corresponding significances of the bZh process with 300 (1000) fb^{-1} integrated luminosity.

reconstructed by anti-k_T algorithm with radius parameter $R = 0.4$. The separation ΔR between any two b-jets, a b-jet and a lepton and between two leptons should be > 0.4. In order to reduce the $t\bar{t}+$jets background, we veto events having missing transverse energy $(E_T^{\rm miss}) > 35\,$GeV. The invariant mass of the two same flavor opposite charge leptons $(m_{\ell\ell})$ is needed to remain between $76 < m_{\ell\ell} < 100\,$GeV, i.e., the Z boson mass window. We then apply invariant mass for two b-jets m_{bb} in a event. As there are at least three b-jets in a event, more than one m_{bb} combinations are possible; the one closest to m_h is selected and

required to remain within $|m_h - m_{bb}| < 25\,\text{GeV}$. Further, we require the invariant mass $m_{\ell\ell bb}$ constructed from the two same flavor opposite charge leptons and b-jets combination that passes the m_{bb} selection to be within $|m_A - m_{\ell\ell bb}| < 50\,\text{GeV}$. The normalized $m_{\ell\ell}$ and m_{bb} distributions before application of any selection cuts are presented in figure 5 while the same for $m_{\ell\ell bb}$ is shown in figure 6. We adopt the b-tagging efficiency and c- and light-jets misidentification efficiencies of Delphes ATLAS based detector card. The background cross sections after selection cuts of the three benchmark points are summarized in table. 3, while the signal cross sections along with their corresponding significances with the integrated luminosity $\mathcal{L} = 300$ and $1000\,\text{fb}^{-1}$ are presented in table 4. The statistical significances are estimated using $\mathcal{Z} = \sqrt{2[(S+B)\ln(1+S/B) - S]}$ [167], where S and B are the numbers of the signal and background events.

Let us take a closer look at table 4. We find very promising the discovery potential with sufficiently large S/B ratio, especially for $m_A < 2m_t$. The achievable significance for the BPa and BPb are $\sim 2.9\sigma$ ($\sim 5.3\sigma$) and $\sim 5.4\sigma$ ($\sim 9.8\sigma$) respectively with 300 (1000) fb^{-1} integrated luminosity. The BPc requires larger dataset due to fall in parton luminosity and suppression from $\mathcal{B}(A \to t\bar{t})$ decay and $\sim 2.2\sigma$ is possible with 1000 fb^{-1} but could reach up to $\sim 3.8\sigma$ with the full high luminosity LHC (HL-LHC) dataset (3000 fb^{-1} integrated luminosity).

4.2 The $bg \to bA \to bt\bar{t}$ process

We now discuss the discovery potential of $pp \to bA + X \to bt\bar{t} + X$, followed by semileptonic decay of at least one top quark, constituting three b-jets, at least one charged lepton (e and μ) and missing transverse energy (E_T^{miss}) signature, which we denote as $3b1\ell$ signature. Note that $bg \to bA \to bt\bar{t}$ is only possible for BPc as $m_A < 2m_t$ but for BPa and BPb one can have $3b1\ell$ signature via $pp \to bH + X \to bt\bar{t} + X$. However, such signatures will be mild for the former two BPs due to suppression from $\mathcal{B}(H \to AZ)$. Further, $bg \to \bar{t}H^+ \to \bar{t}t\bar{b}$ process may also contribute to the same final state topologies, if at least one of the top decays semileptonically. Such contribution could be moderate for all three BPs. In our analysis, however, we neglect them for simplicity.

There exist several SM backgrounds. The dominant backgrounds are $t\bar{t}$+jets, t- and s-channel single-top (tj), Wt, with subdominant backgrounds from $t\bar{t}h$ and, $t\bar{t}Z$ productions. Further, small contributions come from Drell-Yan+jets, W+jets, four-top ($4t$), $t\bar{t}W$, tWh, which are collectively denoted as "Others". We do not include backgrounds originating from non-prompt and fake sources. These backgrounds are not properly modeled in Monte Carlo event generators and one requires data to estimate such contributions.

Here we follow the same event generation procedure for signal and backgrounds as in previous subsections, i.e., via MadGraph5_aMC followed by hadronization and showering in Pythia and with Delphes ATLAS based detector card for fast detector simulation. The LO $t\bar{t}$+jets background cross section is normalized up to the NNLO by a factor of 1.84 while t- and s-channel single-top cross sections are normalized by factors of 1.2 and 1.47, respectively [166]. The LO Wt+jets background is normalized to the NLO cross section by a factor of 1.35, whereas the subdominant $t\bar{t}h$ and $t\bar{t}Z$ are corrected to corresponding NLO ones by factors of 1.27 and 1.56 respectively. The DY+jets background is normalized
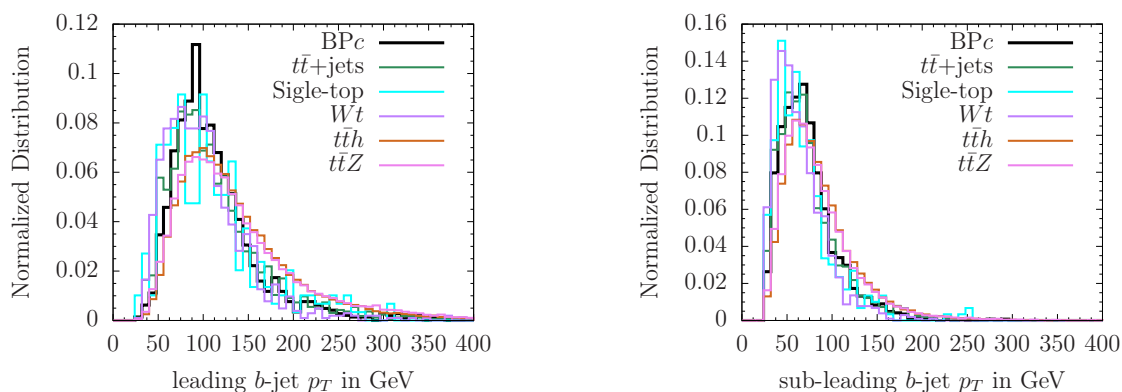
Figure 7. The normalized p_T distributions of the leading and subleading b-jets for the signal (BPc) and the leading backgrounds.
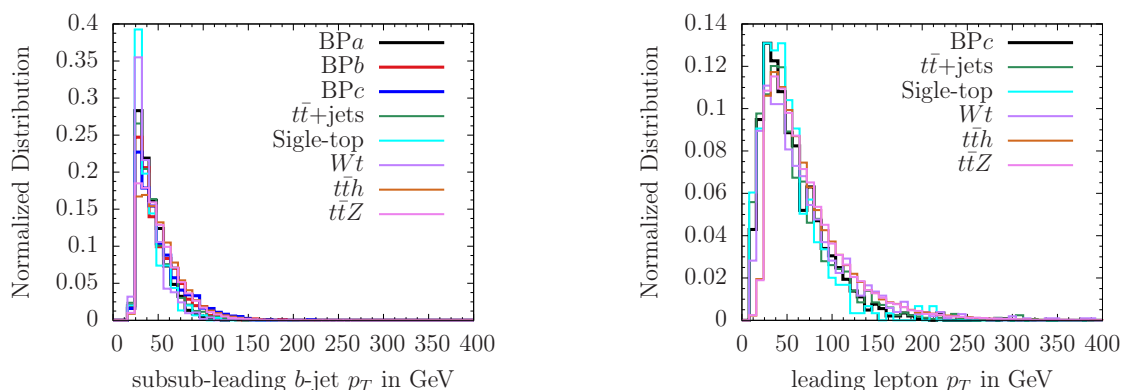

Figure 8. The normalized p_T distributions of the subsubleading b-jet (right) and leading lepton (left) for the signal (BPc) and leading backgrounds.

to NNLO cross sections by factor of 1.27. Finally, the LO cross sections $4t$ and $t\bar{t}W$ are adjusted to the NLO ones by factors of 2.04 and 1.35, respectively. The tWh and W+jets background are kept at LO. For simplicity we assume the correction factors for the charge conjugate processes to be the same. We remark that the signal cross sections for all the three BPs are kept at LO.

The events are selected in a way such that they should contain at least one charged lepton (e and μ), at least three b-tagged and some E_T^{miss}. The normalized transverse momentum (p_T) distributions of the leading and subleading b-jets for the signal and leading backgrounds are presented in figure 7. The p_T distributions for the subsubleading b-jet and leading lepton are plotted in figure 8, while the normalized E_T^{miss} and H_T (i.e., the scalar sum of p_T of the leading charged lepton and the three leading b-jets) distributions are shown in figure 9. To reduce backgrounds we apply the following event selection cuts. p_T of all three b-jets should be $p_T > 20\,\text{GeV}$, whereas that of the leading lepton should be $p_T > 25\,\text{GeV}$. The absolute value of pseudo-rapidity ($|\eta|$) of all three b-jets and lepton should be less than 2.5. The minimum separation (ΔR) between the lepton and any b-jet as well
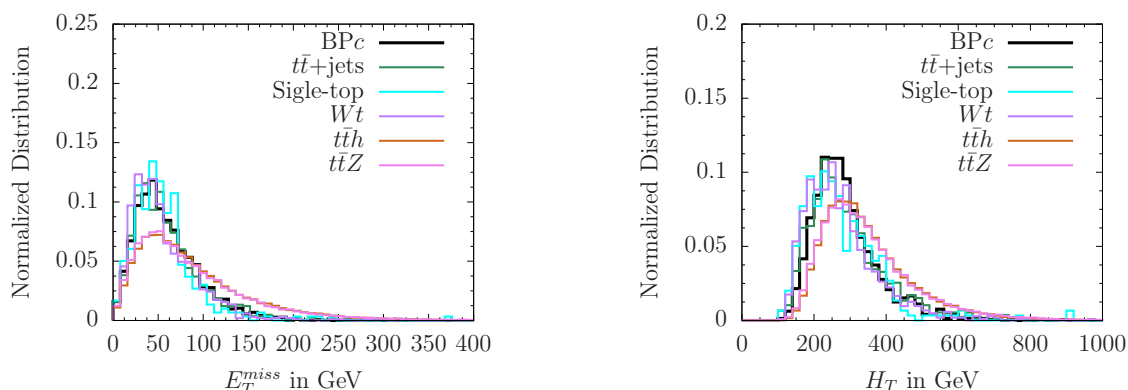
Figure 9. The normalized missing energy E_T^{miss} (left) and H_T (right) for the signal (BPc) and leading backgrounds.

BP	Signal	$t\bar{t}+$ jets	Single-top	$Wt+$ jets	$t\bar{t}h$	$t\bar{t}Z$	Others	Total Bkg. (fb)
BPc	9.27	3953.49	98.93	77.93	10.72	4.13	30.85	4176.05

Table 5. The cross sections (in units of fb) of the signal (BPc) and different background components for $3b1\ell$ process after selection cuts at $\sqrt{s} = 14\,\mathrm{TeV}$.

as that between any two b-jets are required to be greater than 0.4. The E_T^{miss} in each event should be larger than $35\,\mathrm{GeV}$. Note that in our exploratory study we do not optimize the selection cuts such as p_T, η, E_T^{miss} and H_T for simplicity. The signal and total background cross sections along with different components after the selection cuts are shown in table 5.

The corresponding significance $\mathcal{Z}$ for the integrated luminosities 300 (3000) fb^{-1} for the BPc is $\sim 3.5\sigma$ ($\sim 7.9\sigma$). For the BPa and BPb from $pp \to bH + X \to bt\bar{t} + X$ are $\sim 2.4\sigma$ and $\sim 2.8\sigma$ respectively for 3000 fb^{-1} . Note that here we have not considered the systematic uncertainties associated with the backgrounds, which could be considerable in particular for the largest $t\bar{t}+$ jets backgrounds. As $S \ll B$ for the $3b1\ell$ process, in the presence of systematic uncertainties the $\mathcal{Z}$ formula simply becomes $\mathcal{Z} \approx S/\sqrt{B + \sigma_B^2}$. The σ_B denotes the systematic uncertainty that depends on the factor between control sample and the background in the signal region. The value of σ_B is very much analysis[15] dependent. Here we assume that the systematic uncertainty arise only from $t\bar{t}+$ jets backgrounds for simplicity and neglect the same for other subdominant backgrounds and take two different for σ_B for illustration. E.g., if $\sigma_B = \sqrt{B}$ the significance of BPc reduces to $\sim 5.5\sigma$ whereas for $\sigma_B = 0.1\,B$ the significances goes below 1σ with HL-LHC dataset. Similarly, for $\sigma_B = \sqrt{B}$ the significances of BPa and BPb from $pp \to bH + X \to bt\bar{t} + X$ reduces to $\sim 1.7\sigma$ and $\sim 2\sigma$ respectively but much below 1σ if $\sigma_B = 0.1\,B$. Therefore we remark that the $3b1\ell$ process is promising, but one needs precise understanding of the background systematics.

---

[15]We thank Efe Yazgan and K.-F. Chen for clarifying this point. We also thank the anonymous reviewer for bringing this issue to our attention.

BP	Signal	$t\bar{t}+$ jets	Single-top	$Wt+$ jets	Others	Total Bkg. (fb)
BPa	0.2	229.2	4.5	2.8	7.8	244.3
BPb	0.14	204.9	4.0	2.3	8.2	219.4
BPc	0.01	157.8	2.7	1.9	5.3	167.7

Table 6. The cross sections (in units of fb) of three BPs and the different background components for the $4b1\ell$ process after selection cuts at $\sqrt{s} = 14$ TeV.

4.3 The $gg \to t\bar{t}A \to t\bar{t}b\bar{b}$ process

We now briefly discuss the discovery potential of $gg \to t\bar{t}A \to t\bar{t}b\bar{b}$ process. The process can in principle probe the parameter space for ρ_{bb}-EWBG mechanism. We search this process via $pp \to t\bar{t}A + X \to t\bar{t}b\bar{b} + X$, followed by at least one top quark decaying semileptonically i.e., with four b-jets, at least one charged lepton and E_T^{miss} signature. The final state topology receives mild contributions from inclusive $pp \to WtA + X$ and $pp \to tjA + X$ processes. As we show below, the signature is not promising as opposed to $bg \to bA \to bt\bar{t}$ process.

We generate events at LO as in $3b1\ell$ process, i.e., via MadGraph5_aMC followed by hadronization and showering in Pythia and finally incorporate the detector effects of Delphes ATLAS based detector card. The dominant backgrounds arise from the $t\bar{t}+$ jets, Single-top and $Wt+$ jets, whereas $t\bar{t}h$, $t\bar{t}Z$ and $4t$ constitute subdominant backgrounds. We assume the same QCD corrections factor as in $3b1\ell$ process for simplicity.

To reduce the background, we use the following event selection cuts. The events are selected so that they contain at least one lepton (e and μ), at least four jets with at least four are b-tagged and some missing E_T^{miss} (denoted as $4b1\ell$ process). The lepton is required to have $p_T > 25$ GeV and $|\eta| < 2.5$. For any jet in the event $p_T > 20$ GeV and $|\eta| < 2.5$. E_T^{miss} in each event is required to be greater than 35 GeV. The separation ΔR between any two jets as well as that between a jet and a lepton should be larger than 0.4. Finally, we construct all possible combinations of the invariant mass m_{jj} from the four leading jets and demand that the one closest to m_A should lie between $|m_A - m_{jj}| < 50$ GeV. The impact of these cuts on the signal and background processes are summarized in table 6.

We find that the achievable significance for all three BPs of the $gg \to t\bar{t}A \to t\bar{t}b\bar{b}$ process are below $\sim 1\sigma$ with 3000 fb^{-1} integrated luminosity, which is rather low. This means that no meaningful constraints can be extracted unless both ATLAS and CMS data are added. It should be remarked that since we use the same QCD correction factors for the backgrounds as in $bg \to bA \to bt\bar{t}$ process, there are greater uncertainties in these cross sections.

Before closing this section, we discuss the impact of the other ρ_{ij} couplings. So far, we have set all $\rho_{ij} = 0$ except ρ_{bb} and ρ_{tt}. Presence of the other ρ_{ij} couplings open up other decay modes of A, which in principle may reduce the achievable significances summarized in previous subsections. For instance, if $\rho_{\tau\tau} \sim \lambda_\tau$, it would induce $A \to \tau^+\tau^-$ decay. However,

the significances remain practically same for all the three BPs. Moreover, $\rho_{tc} \sim 0.3$-0.4 is still allowed by current data and would induce $cg \to tA/tH \to tt\bar{c}$ (same-sign top) [93, 168] (see also refs. [169, 170][16]) and $cg \to tA/tH \to tt\bar{c}$ (triple-top) signature, which might emerge in the Run-3 of LHC.

5 Discussion and summary

We have analyzed the available constraints and prospect of probing EWBG driven by the extra bottom Yukawa coupling ρ_{bb} at the ongoing and future experiments. The parameter space receives meaningful constraints from h boson coupling measurements, $\mathcal{B}(B \to X_s\gamma)$, $\Delta\mathcal{A}_{CP}$ of $B \to X_s\gamma$, electron EDM measurement and heavy Higgs searches at the LHC. We primarily focused on sub-TeV m_A, m_H and $m_{H^\pm}$ with mixing angle $c_\gamma \sim 0.1$, which is required by EWBG [15–77, 85]. The constraints would be improved, e.g., on c_γ, ρ_{bb} and ρ_{tt} at the HL-LHC [85, 174] if no discovery is made. This would allow us to probe even larger part of the parameter space of ρ_{bb}-EWBG.

Taking three benchmark points for illustration, two below $2m_t$ threshold and one above, we have shown that a discovery is possible at the LHC via ρ_{bb} induced $bg \to bA \to bZh$ process for $m_A < 2m_t$. We find that the process may emerge in the Run 3 of LHC if $250\,\text{GeV} \lesssim m_A \lesssim 350\,\text{GeV}$. With a simple rescaling of the significances in table 4, we find that $|\text{Im}(\rho_{bb})| \gtrsim 0.05$ and $\gtrsim 0.04$ can be excluded for BPa and BPb with full HL-LHC dataset. Those are below the nominal value $|\text{Im}(\rho_{bb})| \gtrsim 0.058$ required EWBG. For $m_A > 2m_t$, a discovery may happen via $bg \to bA \to bt\bar{t}$. Note that one may also have the $bg \to bH \to bhh$ process, which could be sensitive if H is lighter than A and $H^\pm$. The process is being studied elsewhere. A discovery of the $bg \to bA \to bt\bar{t}$ process is possible via $3b1\ell$ signature if $m_A \sim 450\,\text{GeV}$ and $\rho_{tt} \sim 0.5$ but requires controlling of the systematics of $t\bar{t}$-jets background. Additionally, we have also investigated the potential for $gg \to t\bar{t}A \to t\bar{t}b\bar{b}$ process but find it below the sensitivity even at the HL-LHC.

In principle the $pp \to bA + X$ process can also be induced by ρ_{bd}, ρ_{db}, ρ_{bs} and ρ_{sb} at the LHC. However, due to severe constraints arising from B_d and B_s mixings [176] their impacts are typically inconsequential. In addition if the charm quark gets misidentified as b-jet, a sizable ρ_{cc} can also mimic similar signature in pp collision via $cg \to cA \to ct\bar{t}$ process. We remark that such possibilities can be disentangled by the simultaneous application of b- and c-tagging on the final state topologies [177].

Although the discovery is possible at the LHC, to attribute it to ρ_{bb}-EWBG mechanism is beyond the scope of LHC as information of the CP-violating phase of ρ_{bb} is lost in pp collision. In this regard, $\Delta\mathcal{A}_{CP}$ of $\mathcal{B}(B \to X_s\gamma)$ would provide very sensitive probe for the $\text{Im}(\rho_{bb})$ even though the observable has uncertainties associated with the hadronic parameter $\tilde{\Lambda}_{78}$. While finding the constraints in figure 2, we assumed $\tilde{\Lambda}_{78} = 89\,\text{MeV}$, which is the average of $17\,\text{MeV} \leq \tilde{\Lambda}_{78} \leq 190\,\text{MeV}$ [130]. However, if $\tilde{\Lambda}_{78}$ is taken as its upper range, the constraint becomes much severe for $\text{Im}(\rho_{bb})$. Furthermore, on the experimental side, projected Belle II accuracy of $\Delta\mathcal{A}_{CP}$ measurement is $\sim 5\%$ [175]. Therefore, more precise estimation of $\tilde{\Lambda}_{78}$ together with Belle II measurement can stringently probe the parameter

---

[16]Without detailed studies, the process was also discussed by [171, 172] and ref. [170]. See also ref. [173].

space of $\mathrm{Im}(\rho_{bb})$ unless the CP-violating phases of ρ_{tt} and ρ_{bb} are aligned [86] in which $\Delta\mathcal{A}_{\mathrm{CP}} = 0$. In such a case, measurements of EDMs play a pivotal role in probing $\mathrm{Im}(\rho_{bb})$.

The unprecedented electron EDM constraint set by ACME Collaboration in 2018 reduces most EWBG scenarios to despair. We updated our previous analysis done in ref. [85] including all the relevant Barr-Zee diagrams. Because of the significant contributions arising from the diagrams involving ρ_{ee}, the cancellation mechanism can be effective. It was found that the electron EDM cancellation in ρ_{bb}-EWBG belongs to the unstructured cancellation category in which the diagonal hierarchical structures of ρ_{ij}^{F} are much different from those of the SM Yukawa couplings, which is in stark contrast to the case in ρ_{tt}-EWBG that can accommodate the structured cancellation [86]. Nonetheless, the viable parameter space of ρ_{bb}-EWBG still exists. Besides the extreme fine tuning of the parameters, ρ_{bb}-EWBG would be confirmed or ruled out if the electron EDM is improved down to $\sim 10^{-30}$ e cm level. Moreover, as discussed in section 3.2, the future measurement of the proton EDM could play a complementary role in probing ρ_{bb}-EWBG.

So far we have not discussed the uncertainties. As a first estimate, uncertainties arising from factorization scale (μ_F) and renormalization scale (μ_R) dependences are not included in our LO cross section estimations. In general, the LO $bg \to bA/bH$ processes have $\sim 25-30\%$ scale uncertainties for $m_{A/H} \sim (300-400)$ GeV if bottom quark with $p_T > (15-30)$ GeV and, $|\eta| < 2.5$ [178] (see also [179–181]). It has been found that [182] the LO cross sections calculated with LO PDF set CTEQ6L1 [183] have relatively higher factorization scale dependence. Therefore, we remark that the LO cross sections in our analysis, which we estimated with LO NN23LO1 PDF set, might have same level of uncertainties. It has also been found that [182] for $\mu_F \approx m_A$ (or m_H) the corrections to the LO cross sections could be large negative ($\sim -70\%$), whereas for the choice of $\mu_F \approx m_A/4$ (or $m_H/4$) the corrections are mild; which indicates that the $\mu_F \approx m_A/4$ is the relevant factorization scale. Furthermore, the cross section uncertainties from factorization scale and renormalization choices are found to be particularly small at $\mu_R = m_A$ and if varied from $\mu_R = m_A/2$ to $\mu_R = 2m_A$, along with $\mu_F = m_A/4$ and varied from $\mu_F = m_A/8$ to $\mu_F = m_A/2$ [182]. In addition, our analysis does not include PDF uncertainties, which could be in general significant for any bottom-quark initiated process as discussed, e.g., in ref. [184]. Detailed discussions on different PDFs and associated uncertainties for the LHC are summarized in ref. [185]. These typically would induce some uncertainties in our results. We leave out the detailed estimation of these uncertainties for future work.

In summary, we have explored the possibility of electroweak baryogenesis induced by the extra bottom Yukawa coupling ρ_{bb} via direct and indirect signatures at the collider experiments. We find that the discovery is possible at the high luminosity LHC if 250 GeV $\lesssim m_A \lesssim 350$ GeV. We also find that heavier mass ranges can also be probed via $bg \to bA \to bt\bar{t}$ but the process is associated with larger uncertainties. While LHC can indeed discover the process, however, the information of the CP-violating phase of ρ_{bb} can only be probed via $\Delta\mathcal{A}_{\mathrm{CP}}$ of $\mathcal{B}(B \to X_s\gamma)$ or the EDM measurements of the electron, neutron and mercury though the latter two have the less probing power to date. For completeness we also studied $gg \to t\bar{t}A \to t\bar{t}b\bar{b}$ process and found that it is not promising. In conclusion, together with the electron EDM measurement and/or $\Delta\mathcal{A}_{\mathrm{CP}}$ of $\mathcal{B}(B \to X_s\gamma)$

decay, the discovery of $bg \to bA \to bt\bar{t}$ process may help us to understand the mechanism behind the observed matter-antimatter asymmetry of the Universe.

Acknowledgments

A EDMs

For the EDM calculations, the following parametrization is also useful.

$$\mathcal{L}_{\phi\bar{f}f} = -\phi\bar{f}(g^S_{\phi\bar{f}f} + i\gamma_5 g^P_{\phi\bar{f}f})f, \tag{A.1}$$

where $\phi = h, H, A$ and

$$g^S_{h\bar{f}f} = \frac{1}{\sqrt{2}}\Big[\lambda_f s_\gamma + \mathrm{Re}\rho_{ff}c_\gamma\Big], \qquad\qquad g^P_{h\bar{f}f} = \frac{1}{\sqrt{2}}\mathrm{Im}\rho_{ff}c_\gamma, \tag{A.2}$$

$$g^S_{H\bar{f}f} = \frac{1}{\sqrt{2}}\Big[\lambda_f c_\gamma - \mathrm{Re}\rho_{ff}s_\gamma\Big], \qquad\qquad g^P_{H\bar{f}f} = -\frac{1}{\sqrt{2}}\mathrm{Im}\rho_{ff}s_\gamma, \tag{A.3}$$

$$g^S_{A\bar{f}f} = \pm\frac{1}{\sqrt{2}}\mathrm{Im}\rho_{ff}, \qquad\qquad g^P_{A\bar{f}f} = \mp\frac{1}{\sqrt{2}}\mathrm{Re}\rho_{ff}, \tag{A.4}$$

where the upper sign is for up-type fermions and the lower for down-type fermions in eq. (A.4).

Here we list the loop functions appearing in the EDM calculations in section 3.2.

$$f(\tau) = \frac{\tau}{2}\int_0^1 dx \, \frac{1 - 2x(1-x)}{x(1-x) - \tau}\ln\left(\frac{x(1-x)}{\tau}\right), \tag{A.5}$$

$$g(\tau) = \frac{\tau}{2}\int_0^1 dx \, \frac{1}{x(1-x) - \tau}\ln\left(\frac{x(1-x)}{\tau}\right), \tag{A.6}$$

$$\begin{aligned} \mathcal{J}^V_W(m_\phi) = \frac{2m_W^2}{m_\phi^2 - m_V^2}\Bigg[&-\frac{1}{4}\left\{\left(6 - \frac{m_V^2}{m_W^2}\right) + \left(1 - \frac{m_V^2}{2m_W^2}\right)\frac{m_\phi^2}{m_W^2}\right\} \\ &\times \left(I_1(m_W, m_\phi) - I_1(m_W, m_V)\right) \\ &+ \left\{\left(-4 + \frac{m_V^2}{m_W^2}\right) + \frac{1}{4}\left(6 - \frac{m_V^2}{m_W^2}\right) + \frac{1}{4}\left(1 - \frac{m_V^2}{2m_W^2}\right)\frac{m_\phi^2}{m_W^2}\right\} \\ &\times \left(I_2(m_W, m_\phi) - I_2(m_W, m_V)\right)\Bigg], \end{aligned} \tag{A.7}$$

$$J_1(\tau_{WH^\pm}, \tau_{tH^\pm}) = \int_0^1 \frac{dx}{x}(2-x)\Big[Q_t(1-x)J\left(\tau_{WH^\pm}, \frac{\tau_{tH^\pm}}{x}\right) + Q_b x J\left(\tau_{WH^\pm}, \frac{\tau_{tH^\pm}}{x}\right)\Big], \tag{A.8}$$

where $\tau_{ij} = m_i^2/m_j^2$, $Q_t = 2/3$, $Q_b = -1/3$ and

$$I_1(m_1, m_2) = -2\frac{m_2^2}{m_1^2}f\left(\frac{m_1^2}{m_2^2}\right), \quad I_2(m_1, m_2) = -2\frac{m_2^2}{m_1^2}g\left(\frac{m_1^2}{m_2^2}\right), \tag{A.9}$$

$$J(a, b) = \frac{1}{a-b}\left[\frac{a}{a-1}\ln a - \frac{b}{b-1}\ln b\right]. \tag{A.10}$$

References

[1] PARTICLE DATA GROUP collaboration, *Review of particle physics*, *Phys. Rev. D* **98** (2018) 030001 [INSPIRE].

[2] A.D. Sakharov, *Violation of CP invariance, C asymmetry and baryon asymmetry of the universe*, *Sov. Phys. Usp.* **34** (1991) 392 [*Pisma Zh. Eksp. Teor. Fiz.* **5** (1967) 32] [*JETP Lett.* **5** (1967) 24] [*Usp. Fiz. Nauk* **161** (1991) 61] [INSPIRE].

[3] ATLAS collaboration, *Observation of a new particle in the search for the Standard Model Higgs boson with the ATLAS detector at the LHC*, *Phys. Lett. B* **716** (2012) 1 [`arXiv:1207.7214`] [INSPIRE].

[4] V.A. Kuzmin, V.A. Rubakov and M.E. Shaposhnikov, *On the anomalous electroweak baryon number nonconservation in the early universe*, *Phys. Lett. B* **155** (1985) 36 [INSPIRE].

[5] M. Quirós, *Field theory at finite temperature and phase transitions*, *Helv. Phys. Acta* **67** (1994) 451 [INSPIRE].

[6] V.A. Rubakov and M.E. Shaposhnikov, *Electroweak baryon number nonconservation in the early universe and in high-energy collisions*, *Usp. Fiz. Nauk* **166** (1996) 493 [*Phys. Usp.* **39** (1996) 461] [`hep-ph/9603208`] [INSPIRE].

[7] K. Funakubo, *CP violation and baryogenesis at the electroweak phase transition*, *Prog. Theor. Phys.* **96** (1996) 475 [`hep-ph/9608358`] [INSPIRE].

[8] A. Riotto, *Theories of baryogenesis*, in *ICTP summer school in high-energy physics and cosmology*, (1998), pg. 326 [`hep-ph/9807454`] [INSPIRE].

[9] M. Trodden, *Electroweak baryogenesis*, *Rev. Mod. Phys.* **71** (1999) 1463 [`hep-ph/9803479`] [INSPIRE].

[10] W. Bernreuther, *CP violation and baryogenesis*, *Lect. Notes Phys.* **591** (2002) 237 [`hep-ph/0205279`] [INSPIRE].

[11] J.M. Cline, *Baryogenesis*, in *Les Houches Summer School — session* 86. *Particle physics and cosmology: the fabric of spacetime*, (2006) [`hep-ph/0609145`] [INSPIRE].

[12] D.E. Morrissey and M.J. Ramsey-Musolf, *Electroweak baryogenesis*, *New J. Phys.* **14** (2012) 125003 [`arXiv:1206.2942`] [INSPIRE].

[13] T. Konstandin, *Quantum transport and electroweak baryogenesis*, *Phys. Usp.* **56** (2013) 747 [*Usp. Fiz. Nauk* **183** (2013) 785] [`arXiv:1302.6713`] [INSPIRE].

[14] E. Senaha, *Symmetry restoration and breaking at finite temperature: an introductory review*, *Symmetry* **12** (2020) 733 [INSPIRE].

[15] A.I. Bochkarev, S.V. Kuzmin and M.E. Shaposhnikov, *Electroweak baryogenesis and the Higgs boson mass problem*, *Phys. Lett. B* **244** (1990) 275 [INSPIRE].

[16] K. Funakubo, A. Kakuto and K. Takenaga, *The effective potential of electroweak theory with two massless Higgs doublets at finite temperature*, *Prog. Theor. Phys.* **91** (1994) 341 [hep-ph/9310267] [INSPIRE].

[17] J.M. Cline and P.-A. Lemieux, *Electroweak phase transition in two Higgs doublet models*, *Phys. Rev. D* **55** (1997) 3873 [hep-ph/9609240] [INSPIRE].

[18] S. Kanemura, Y. Okada and E. Senaha, *Electroweak baryogenesis and quantum corrections to the triple Higgs boson coupling*, *Phys. Lett. B* **606** (2005) 361 [hep-ph/0411354] [INSPIRE].

[19] L. Fromme, S.J. Huber and M. Seniuch, *Baryogenesis in the two-Higgs doublet model*, *JHEP* **11** (2006) 038 [hep-ph/0605242] [INSPIRE].

[20] T.A. Chowdhury, M. Nemevšek, G. Senjanović and Y. Zhang, *Dark matter as the trigger of strong electroweak phase transition*, *JCAP* **02** (2012) 029 [arXiv:1110.5334] [INSPIRE].

[21] D. Borah and J.M. Cline, *Inert doublet dark matter with strong electroweak phase transition*, *Phys. Rev. D* **86** (2012) 055001 [arXiv:1204.4722] [INSPIRE].

[22] J.M. Cline and K. Kainulainen, *Improved electroweak phase transition with subdominant inert doublet dark matter*, *Phys. Rev. D* **87** (2013) 071701 [arXiv:1302.2614] [INSPIRE].

[23] G. Gil, P. Chankowski and M. Krawczyk, *Inert dark matter and strong electroweak phase transition*, *Phys. Lett. B* **717** (2012) 396 [arXiv:1207.0084] [INSPIRE].

[24] G.C. Dorsch, S.J. Huber and J.M. No, *A strong electroweak phase transition in the 2HDM after LHC8*, *JHEP* **10** (2013) 029 [arXiv:1305.6610] [INSPIRE].

[25] G.C. Dorsch, S.J. Huber, K. Mimasu and J.M. No, *Echoes of the electroweak phase transition: discovering a second Higgs doublet through $A_0 \to ZH_0$*, *Phys. Rev. Lett.* **113** (2014) 211802 [arXiv:1405.5537] [INSPIRE].

[26] N. Blinov, S. Profumo and T. Stefaniak, *The electroweak phase transition in the inert doublet model*, *JCAP* **07** (2015) 028 [arXiv:1504.05949] [INSPIRE].

[27] K. Fuyuto and E. Senaha, *Sphaleron and critical bubble in the scale invariant two Higgs doublet model*, *Phys. Lett. B* **747** (2015) 152 [arXiv:1504.04291] [INSPIRE].

[28] K. Fuyuto, J. Hisano and E. Senaha, *Toward verification of electroweak baryogenesis by electric dipole moments*, *Phys. Lett. B* **755** (2016) 491 [arXiv:1510.04485] [INSPIRE].

[29] P. Basler, M. Mühlleitner and J. Wittbrodt, *The CP-violating 2HDM in light of a strong first order electroweak phase transition and implications for Higgs pair production*, *JHEP* **03** (2018) 061 [arXiv:1711.04097] [INSPIRE].

[30] K. Kainulainen, V. Keus, L. Niemi, K. Rummukainen, T.V.I. Tenkanen and V. Vaskonen, *On the validity of perturbative studies of the electroweak phase transition in the two Higgs doublet model*, *JHEP* **06** (2019) 075 [arXiv:1904.01329] [INSPIRE].

[31] E. Senaha, *Radiative corrections to triple Higgs coupling and electroweak phase transition: beyond one-loop analysis*, *Phys. Rev. D* **100** (2019) 055034 [arXiv:1811.00336] [INSPIRE].

[32] F.P. Huang and E. Senaha, *Enhanced Z boson decays as a new probe of first-order electroweak phase transition at future lepton colliders*, *Phys. Rev. D* **100** (2019) 035014 [arXiv:1905.10283] [INSPIRE].

[33] X. Wang, F.P. Huang and X. Zhang, *Gravitational wave and collider signals in complex two-Higgs doublet model with dynamical CP-violation at finite temperature*, *Phys. Rev. D* **101** (2020) 015015 [arXiv:1909.02978] [InSPIRE].

[34] M. Pietroni, *The electroweak phase transition in a nonminimal supersymmetric model*, *Nucl. Phys. B* **402** (1993) 27 [hep-ph/9207227] [InSPIRE].

[35] J.R. Espinosa, M. Quirós and F. Zwirner, *On the electroweak phase transition in the minimal supersymmetric Standard Model*, *Phys. Lett. B* **307** (1993) 106 [hep-ph/9303317] [InSPIRE].

[36] A. Brignole, J.R. Espinosa, M. Quirós and F. Zwirner, *Aspects of the electroweak phase transition in the minimal supersymmetric Standard Model*, *Phys. Lett. B* **324** (1994) 181 [hep-ph/9312296] [InSPIRE].

[37] A.T. Davies, C.D. Froggatt and R.G. Moorhouse, *Electroweak baryogenesis in the next-to-minimal supersymmetric model*, *Phys. Lett. B* **372** (1996) 88 [hep-ph/9603388] [InSPIRE].

[38] J.R. Espinosa, *Dominant two loop corrections to the MSSM finite temperature effective potential*, *Nucl. Phys. B* **475** (1996) 273 [hep-ph/9604320] [InSPIRE].

[39] B. de Carlos and J.R. Espinosa, *The baryogenesis window in the MSSM*, *Nucl. Phys. B* **503** (1997) 24 [hep-ph/9703212] [InSPIRE].

[40] S.J. Huber and M.G. Schmidt, *Electroweak baryogenesis: concrete in a SUSY model with a gauge singlet*, *Nucl. Phys. B* **606** (2001) 183 [hep-ph/0003122] [InSPIRE].

[41] K. Funakubo, S. Tao and F. Toyoda, *CP violation in the Higgs sector and phase transition in the MSSM*, *Prog. Theor. Phys.* **109** (2003) 415 [hep-ph/0211238] [InSPIRE].

[42] K. Funakubo, S. Tao and F. Toyoda, *Phase transitions in the NMSSM*, *Prog. Theor. Phys.* **114** (2005) 369 [hep-ph/0501052] [InSPIRE].

[43] S.J. Huber, T. Konstandin, T. Prokopec and M.G. Schmidt, *Electroweak phase transition and baryogenesis in the NMSSM*, *Nucl. Phys. B* **757** (2006) 172 [hep-ph/0606298] [InSPIRE].

[44] K. Funakubo and E. Senaha, *Electroweak phase transition, critical bubbles and sphaleron decoupling condition in the MSSM*, *Phys. Rev. D* **79** (2009) 115024 [arXiv:0905.2022] [InSPIRE].

[45] C.-W. Chiang and E. Senaha, *Electroweak phase transitions in the secluded* U(1)′-*extended MSSM*, *JHEP* **06** (2010) 030 [arXiv:0912.5069] [InSPIRE].

[46] D.J.H. Chung and A.J. Long, *Electroweak phase transition in the* $\mu\nu$*SSM*, *Phys. Rev. D* **81** (2010) 123531 [arXiv:1004.0942] [InSPIRE].

[47] S. Kanemura, E. Senaha and T. Shindou, *First-order electroweak phase transition powered by additional F-term loop effects in an extended supersymmetric Higgs sector*, *Phys. Lett. B* **706** (2011) 40 [arXiv:1109.5226] [InSPIRE].

[48] M. Carena, N.R. Shah and C.E.M. Wagner, *Light dark matter and the electroweak phase transition in the NMSSM*, *Phys. Rev. D* **85** (2012) 036003 [arXiv:1110.4378] [InSPIRE].

[49] K. Cheung, T.-J. Hou, J.S. Lee and E. Senaha, *Singlino-driven electroweak baryogenesis in the next-to-MSSM*, *Phys. Lett. B* **710** (2012) 188 [arXiv:1201.3781] [InSPIRE].

[50] R. Fok, G.D. Kribs, A. Martin and Y. Tsai, *Electroweak baryogenesis in R-symmetric supersymmetry*, *Phys. Rev. D* **87** (2013) 055018 [arXiv:1208.2784] [INSPIRE].

[51] S. Kanemura, E. Senaha, T. Shindou and T. Yamada, *Electroweak phase transition and Higgs boson couplings in the model based on supersymmetric strong dynamics*, *JHEP* **05** (2013) 066 [arXiv:1211.5883] [INSPIRE].

[52] E. Senaha, *Z′-ino-driven electroweak baryogenesis in the UMSSM*, *Phys. Rev. D* **88** (2013) 055014 [arXiv:1308.3389] [INSPIRE].

[53] J. Kozaczuk, S. Profumo, L.S. Haskins and C.L. Wainwright, *Cosmological phase transitions and their properties in the NMSSM*, *JHEP* **01** (2015) 144 [arXiv:1407.4134] [INSPIRE].

[54] P. Athron, C. Balázs, A. Fowlie, G. Pozzo, G. White and Y. Zhang, *Strong first-order phase transitions in the NMSSM — a comprehensive survey*, *JHEP* **11** (2019) 151 [arXiv:1908.11847] [INSPIRE].

[55] J. Choi and R.R. Volkas, *Real Higgs singlet and the electroweak phase transition in the Standard Model*, *Phys. Lett. B* **317** (1993) 385 [hep-ph/9308234] [INSPIRE].

[56] S.W. Ham, Y.S. Jeong and S.K. Oh, *Electroweak phase transition in an extension of the Standard Model with a real Higgs singlet*, *J. Phys. G* **31** (2005) 857 [hep-ph/0411352] [INSPIRE].

[57] A. Ahriche, *What is the criterion for a strong first order electroweak phase transition in singlet models?*, *Phys. Rev. D* **75** (2007) 083522 [hep-ph/0701192] [INSPIRE].

[58] S. Profumo, M.J. Ramsey-Musolf and G. Shaughnessy, *Singlet Higgs phenomenology and the electroweak phase transition*, *JHEP* **08** (2007) 010 [arXiv:0705.2425] [INSPIRE].

[59] J.R. Espinosa and M. Quirós, *Novel effects in electroweak breaking from a hidden sector*, *Phys. Rev. D* **76** (2007) 076004 [hep-ph/0701145] [INSPIRE].

[60] A. Ashoorioon and T. Konstandin, *Strong electroweak phase transitions without collider traces*, *JHEP* **07** (2009) 086 [arXiv:0904.0353] [INSPIRE].

[61] D.J.H. Chung and A.J. Long, *Cosmological constant, dark matter and electroweak phase transition*, *Phys. Rev. D* **84** (2011) 103513 [arXiv:1108.5193] [INSPIRE].

[62] J.R. Espinosa, T. Konstandin and F. Riva, *Strong electroweak phase transitions in the Standard Model with a singlet*, *Nucl. Phys. B* **854** (2012) 592 [arXiv:1107.5441] [INSPIRE].

[63] J.R. Espinosa, B. Gripaios, T. Konstandin and F. Riva, *Electroweak baryogenesis in non-minimal composite Higgs models*, *JCAP* **01** (2012) 012 [arXiv:1110.2876] [INSPIRE].

[64] J.M. Cline and K. Kainulainen, *Electroweak baryogenesis and dark matter from a singlet Higgs*, *JCAP* **01** (2013) 012 [arXiv:1210.4196] [INSPIRE].

[65] J.M. Cline, K. Kainulainen, P. Scott and C. Weniger, *Update on scalar singlet dark matter*, *Phys. Rev. D* **88** (2013) 055025 [*Erratum ibid.* **92** (2015) 039906] [arXiv:1306.4710] [INSPIRE].

[66] K. Fuyuto and E. Senaha, *Improved sphaleron decoupling condition and the Higgs coupling constants in the real singlet-extended Standard Model*, *Phys. Rev. D* **90** (2014) 015015 [arXiv:1406.0433] [INSPIRE].

[67] T. Alanne, K. Tuominen and V. Vaskonen, *Strong phase transition, dark matter and vacuum stability from simple hidden sectors*, *Nucl. Phys. B* **889** (2014) 692 [arXiv:1407.0688] [INSPIRE].

[68] S. Profumo, M.J. Ramsey-Musolf, C.L. Wainwright and P. Winslow, *Singlet-catalyzed electroweak phase transitions and precision Higgs boson studies*, *Phys. Rev. D* **91** (2015) 035018 [arXiv:1407.5342] [INSPIRE].

[69] D. Curtin, P. Meade and C.-T. Yu, *Testing electroweak baryogenesis with future colliders*, *JHEP* **11** (2014) 127 [arXiv:1409.0005] [INSPIRE].

[70] J. Kozaczuk, *Bubble expansion and the viability of singlet-driven electroweak baryogenesis*, *JHEP* **10** (2015) 135 [arXiv:1506.04741] [INSPIRE].

[71] V. Vaskonen, *Electroweak baryogenesis and gravitational waves from a real scalar singlet*, *Phys. Rev. D* **95** (2017) 123515 [arXiv:1611.02073] [INSPIRE].

[72] D. Curtin, P. Meade and H. Ramani, *Thermal resummation and phase transitions*, *Eur. Phys. J. C* **78** (2018) 787 [arXiv:1612.00466] [INSPIRE].

[73] G. Kurup and M. Perelstein, *Dynamics of electroweak phase transition in singlet-scalar extension of the Standard Model*, *Phys. Rev. D* **96** (2017) 015036 [arXiv:1704.03381] [INSPIRE].

[74] C.-W. Chiang, M.J. Ramsey-Musolf and E. Senaha, *Standard Model with a complex scalar singlet: cosmological implications and theoretical considerations*, *Phys. Rev. D* **97** (2018) 015005 [arXiv:1707.09960] [INSPIRE].

[75] F.P. Huang, Z. Qian and M. Zhang, *Exploring dynamical CP-violation induced baryogenesis by gravitational waves and colliders*, *Phys. Rev. D* **98** (2018) 015014 [arXiv:1804.06813] [INSPIRE].

[76] C.-W. Chiang, Y.-T. Li and E. Senaha, *Revisiting electroweak phase transition in the Standard Model with a real singlet scalar*, *Phys. Lett. B* **789** (2019) 154 [arXiv:1808.01098] [INSPIRE].

[77] A. Beniwal, M. Lewicki, M. White and A.G. Williams, *Gravitational waves and electroweak baryogenesis in a global study of the extended scalar singlet model*, *JHEP* **02** (2019) 183 [arXiv:1810.02380] [INSPIRE].

[78] M. Chala, M. Ramos and M. Spannowsky, *Gravitational wave and collider probes of a triplet Higgs sector with a low cutoff*, *Eur. Phys. J. C* **79** (2019) 156 [arXiv:1812.01901] [INSPIRE].

[79] S. Tulin and P. Winslow, *Anomalous B meson mixing and baryogenesis*, *Phys. Rev. D* **84** (2011) 034013 [arXiv:1105.2848] [INSPIRE].

[80] J.M. Cline, K. Kainulainen and M. Trott, *Electroweak baryogenesis in two Higgs doublet models and B meson anomalies*, *JHEP* **11** (2011) 089 [arXiv:1107.3559] [INSPIRE].

[81] T. Liu, M.J. Ramsey-Musolf and J. Shu, *Electroweak beautygenesis: from $b \to s$ CP-violation to the cosmic baryon asymmetry*, *Phys. Rev. Lett.* **108** (2012) 221301 [arXiv:1109.4145] [INSPIRE].

[82] C.-W. Chiang, K. Fuyuto and E. Senaha, *Electroweak baryogenesis with lepton flavor violation*, *Phys. Lett. B* **762** (2016) 315 [arXiv:1607.07316] [INSPIRE].

[83] H.-K. Guo, Y.-Y. Li, T. Liu, M. Ramsey-Musolf and J. Shu, *Lepton-flavored electroweak baryogenesis*, *Phys. Rev. D* **96** (2017) 115034 [arXiv:1609.09849] [INSPIRE].

[84] K. Fuyuto, W.-S. Hou and E. Senaha, *Electroweak baryogenesis driven by extra top Yukawa couplings*, *Phys. Lett. B* **776** (2018) 402 [arXiv:1705.05034] [INSPIRE].

[85] T. Modak and E. Senaha, *Electroweak baryogenesis via bottom transport*, *Phys. Rev. D* **99** (2019) 115022 [arXiv:1811.08088] [inSPIRE].

[86] K. Fuyuto, W.-S. Hou and E. Senaha, *Cancellation mechanism for the electron electric dipole moment connected with the baryon asymmetry of the universe*, *Phys. Rev. D* **101** (2020) 011901 [arXiv:1910.12404] [inSPIRE].

[87] K. Ishikawa, T. Kitahara and M. Takimoto, *Towards a scale free electroweak baryogenesis*, *Phys. Rev. D* **91** (2015) 055004 [arXiv:1410.5432] [inSPIRE].

[88] I. Baldes and G. Servant, *High scale electroweak phase transition: baryogenesis & symmetry non-restoration*, *JHEP* **10** (2018) 053 [arXiv:1807.08770] [inSPIRE].

[89] O. Matsedonskyi and G. Servant, *High-temperature electroweak symmetry non-restoration from new fermions and implications for baryogenesis*, *JHEP* **09** (2020) 012 [arXiv:2002.05174] [inSPIRE].

[90] A. Djouadi, *The anatomy of electro-weak symmetry breaking. I: the Higgs boson in the Standard Model*, *Phys. Rept.* **457** (2008) 1 [hep-ph/0503172] [inSPIRE].

[91] G.C. Branco, P.M. Ferreira, L. Lavoura, M.N. Rebelo, M. Sher and J.P. Silva, *Theory and phenomenology of two-Higgs-doublet models*, *Phys. Rept.* **516** (2012) 1 [arXiv:1106.0034] [inSPIRE].

[92] N. Cabibbo, *Unitary symmetry and leptonic decays*, *Phys. Rev. Lett.* **10** (1963) 531 [inSPIRE].

[93] M. Kohda, T. Modak and W.-S. Hou, *Searching for new scalar bosons via triple-top signature in $cg \to tS^0 \to t t \bar{t}$*, *Phys. Lett. B* **776** (2018) 379 [arXiv:1710.07260] [inSPIRE].

[94] T. Modak, *Probing an additional bottom Yukawa coupling via $bg \to bA \to bZH$ signature*, *Phys. Rev. D* **100** (2019) 035018 [arXiv:1905.02137] [inSPIRE].

[95] S. Davidson and H.E. Haber, *Basis-independent methods for the two-Higgs-doublet model*, *Phys. Rev. D* **72** (2005) 035004 [*Erratum ibid.* **72** (2005) 099902] [hep-ph/0504050] [inSPIRE].

[96] W.-S. Hou and M. Kikuchi, *Approximate alignment in two Higgs doublet model with extra Yukawa couplings*, *EPL* **123** (2018) 11001 [arXiv:1706.07694] [inSPIRE].

[97] ATLAS collaboration, *Search for heavy resonances decaying into a W or Z boson and a Higgs boson in final states with leptons and b-jets in $36\,fb^{-1}$ of $\sqrt{s} = 13\,TeV$ pp collisions with the ATLAS detector*, *JHEP* **03** (2018) 174 [*Erratum ibid.* **11** (2018) 051] [arXiv:1712.06518] [inSPIRE].

[98] CMS collaboration, *Search for a heavy pseudoscalar boson decaying to a Z and a Higgs boson at $\sqrt{s} = 13\,TeV$*, *Eur. Phys. J. C* **79** (2019) 564 [arXiv:1903.00941] [inSPIRE].

[99] P.M. Ferreira, S. Liebler and J. Wittbrodt, *$pp \to A \to Zh$ and the wrong-sign limit of the two-Higgs-doublet model*, *Phys. Rev. D* **97** (2018) 055008 [arXiv:1711.00024] [inSPIRE].

[100] N.M. Coyle, B. Li and C.E.M. Wagner, *Wrong sign bottom Yukawa coupling in low energy supersymmetry*, *Phys. Rev. D* **97** (2018) 115028 [arXiv:1802.09122] [inSPIRE].

[101] A. Djouadi, L. Maiani, A. Polosa, J. Quevillon and V. Riquer, *Fully covering the MSSM Higgs sector at the LHC*, *JHEP* **06** (2015) 168 [arXiv:1502.05653] [inSPIRE].

[102] N. Craig, F. D'Eramo, P. Draper, S. Thomas and H. Zhang, *The hunt for the rest of the Higgs bosons*, *JHEP* **06** (2015) 137 [arXiv:1504.04630] [inSPIRE].

[103] J. Hajer, Y.-Y. Li, T. Liu and J.F.H. Shiu, *Heavy Higgs bosons at 14 TeV and 100 TeV*, *JHEP* **11** (2015) 124 [arXiv:1504.07617] [INSPIRE].

[104] E. Alvarez and M. Estevez, *$t\bar{t}b\bar{b}$ as a probe of new physics at the LHC*, *Phys. Rev. D* **96** (2017) 035016 [arXiv:1701.04427] [INSPIRE].

[105] S. Gori, I.-W. Kim, N.R. Shah and K.M. Zurek, *Closing the wedge: search strategies for extended Higgs sectors with heavy flavor final states*, *Phys. Rev. D* **93** (2016) 075038 [arXiv:1602.02782] [INSPIRE].

[106] ATLAS collaboration, *Search for heavy Higgs bosons A/H decaying to a top quark pair in pp collisions at $\sqrt{s} = 8$ TeV with the ATLAS detector*, *Phys. Rev. Lett.* **119** (2017) 191803 [arXiv:1707.06025] [INSPIRE].

[107] CMS collaboration, *Search for heavy Higgs bosons decaying to a top quark pair in proton-proton collisions at $\sqrt{s} = 13$ TeV*, *JHEP* **04** (2020) 171 [arXiv:1908.01115] [INSPIRE].

[108] M. Carena and Z. Liu, *Challenges and opportunities for heavy scalar searches in the $t\bar{t}$ channel at the LHC*, *JHEP* **11** (2016) 159 [arXiv:1608.07282] [INSPIRE].

[109] S. Kanemura, H. Yokoya and Y.-J. Zheng, *Searches for additional Higgs bosons in multi-top-quarks events at the LHC and the International Linear Collider*, *Nucl. Phys. B* **898** (2015) 286 [arXiv:1505.01089] [INSPIRE].

[110] N. Craig, J. Hajer, Y.-Y. Li, T. Liu and H. Zhang, *Heavy Higgs bosons at low $\tan\beta$: from the LHC to 100 TeV*, *JHEP* **01** (2017) 018 [arXiv:1605.08744] [INSPIRE].

[111] W.-S. Hou, M. Kohda and T. Modak, *Implications of four-top and top-pair studies on triple-top production*, *Phys. Lett. B* **798** (2019) 134953 [arXiv:1906.09703] [INSPIRE].

[112] D. Eriksson, J. Rathsman and O. Stal, *2HDMC: two-Higgs-doublet model calculator physics and manual*, *Comput. Phys. Commun.* **181** (2010) 189 [arXiv:0902.0851] [INSPIRE].

[113] M.E. Peskin and T. Takeuchi, *Estimation of oblique electroweak corrections*, *Phys. Rev. D* **46** (1992) 381 [INSPIRE].

[114] C.D. Froggatt, R.G. Moorhouse and I.G. Knowles, *Leading radiative corrections in two scalar doublet models*, *Phys. Rev. D* **45** (1992) 2471 [INSPIRE].

[115] H.E. Haber and O. Stål, *New LHC benchmarks for the CP-conserving two-Higgs-doublet model*, *Eur. Phys. J. C* **75** (2015) 491 [*Erratum ibid.* **76** (2016) 312] [arXiv:1507.04281] [INSPIRE].

[116] GFITTER GROUP collaboration, *The global electroweak fit at NNLO and prospects for the LHC and ILC*, *Eur. Phys. J. C* **74** (2014) 3046 [arXiv:1407.3792] [INSPIRE].

[117] *Gfitter website*, http://project-gfitter.web.cern.ch/project-gfitter/Oblique_Parameters/.

[118] W.-S. Hou, M. Kohda and T. Modak, *Top-assisted di-Higgs boson production motivated by baryogenesis*, *Phys. Rev. D* **99** (2019) 055046 [arXiv:1901.00105] [INSPIRE].

[119] W.-S. Hou and T. Modak, *Prospects for tZH and tZh production at the LHC*, *Phys. Rev. D* **101** (2020) 035007 [arXiv:1911.06010] [INSPIRE].

[120] M. Ciuchini, G. Degrassi, P. Gambino and G.F. Giudice, *Next-to-leading QCD corrections to $B \to X_s\gamma$: Standard Model and two Higgs doublet model*, *Nucl. Phys. B* **527** (1998) 21 [hep-ph/9710335] [INSPIRE].

[121] K.G. Chetyrkin, M. Misiak and M. Münz, *Weak radiative B meson decay beyond leading logarithms*, *Phys. Lett. B* **400** (1997) 206 [*Erratum ibid.* **425** (1998) 414] [`hep-ph/9612313`] [INSPIRE].

[122] B. Altunkaynak, W.-S. Hou, C. Kao, M. Kohda and B. McCoy, *Flavor changing heavy Higgs interactions at the LHC*, *Phys. Lett. B* **751** (2015) 135 [`arXiv:1506.00651`] [INSPIRE].

[123] HFLAV collaboration, *Averages of b-hadron, c-hadron, and τ-lepton properties as of summer* 2016, *Eur. Phys. J. C* **77** (2017) 895 [`arXiv:1612.07233`] [INSPIRE].

[124] M. Czakon, P. Fiedler, T. Huber, M. Misiak, T. Schutzmeier and M. Steinhauser, *The* $(Q_7, Q_{1,2})$ *contribution to* $\bar{B} \to X_s \gamma$ *at* $O\left(\alpha_s^2\right)$, *JHEP* **04** (2015) 168 [`arXiv:1503.01791`] [INSPIRE].

[125] A. Crivellin, A. Kokulu and C. Greub, *Flavor-phenomenology of two-Higgs-doublet models with generic Yukawa structure*, *Phys. Rev. D* **87** (2013) 094031 [`arXiv:1303.5877`] [INSPIRE].

[126] C.-Q. Geng and J.-N. Ng, *Charged Higgs effect in* B_d^0-$\bar{B}_d^0$ *mixing,* $K \to \pi\nu\bar{\nu}$ *decay and rare decays of B mesons*, *Phys. Rev. D* **38** (1988) 2857 [*Erratum ibid.* **41** (1990) 1715] [INSPIRE].

[127] UTFIT collaboration, *Constraints on new physics from the quark mixing unitarity triangle*, *Phys. Rev. Lett.* **97** (2006) 151803 [`hep-ph/0605213`] [INSPIRE].

[128] *New physics fit results: summer* 2018 *webpage*, http://www.utfit.org/UTfit/ResultsSummer2018NP.

[129] A.L. Kagan and M. Neubert, *Direct CP-violation in* $B \to X_s \gamma$ *decays as a signature of new physics*, *Phys. Rev. D* **58** (1998) 094012 [`hep-ph/9803368`] [INSPIRE].

[130] M. Benzke, S.J. Lee, M. Neubert and G. Paz, *Long-distance dominance of the CP asymmetry in* $B \to X_{s,d} + \gamma$ *decays*, *Phys. Rev. Lett.* **106** (2011) 141801 [`arXiv:1012.3167`] [INSPIRE].

[131] BELLE collaboration, *Measurements of isospin asymmetry and difference of direct CP asymmetries in inclusive* $B \to X_s \gamma$ *decays*, *Phys. Rev. D* **99** (2019) 032012 [`arXiv:1807.04236`] [INSPIRE].

[132] K. Fuyuto, M. Ramsey-Musolf and T. Shen, *Electric dipole moments from CP-violating scalar leptoquark interactions*, *Phys. Lett. B* **788** (2019) 52 [`arXiv:1804.01137`] [INSPIRE].

[133] T. Abe, J. Hisano, T. Kitahara and K. Tobioka, *Gauge invariant Barr-Zee type contributions to fermionic EDMs in the two-Higgs doublet models*, *JHEP* **01** (2014) 106 [*Erratum ibid.* **04** (2016) 161] [`arXiv:1311.4704`] [INSPIRE].

[134] D. Bowser-Chao, D. Chang and W.-Y. Keung, *Electron electric dipole moment from CP-violation in the charged Higgs sector*, *Phys. Rev. Lett.* **79** (1997) 1988 [`hep-ph/9703435`] [INSPIRE].

[135] M. Kobayashi and T. Maskawa, *CP violation in the renormalizable theory of weak interaction*, *Prog. Theor. Phys.* **49** (1973) 652 [INSPIRE].

[136] W. Dekens, J. de Vries, M. Jung and K.K. Vos, *The phenomenology of electric dipole moments in models of scalar leptoquarks*, *JHEP* **01** (2019) 069 [`arXiv:1809.09114`] [INSPIRE].

[137] NEDM collaboration, *Measurement of the permanent electric dipole moment of the neutron*, *Phys. Rev. Lett.* **124** (2020) 081803 [`arXiv:2001.11966`] [INSPIRE].

[138] B. Graner, Y. Chen, E.G. Lindahl and B.R. Heckel, *Reduced limit on the permanent electric dipole moment of* ^{199}Hg, *Phys. Rev. Lett.* **116** (2016) 161601 [*Erratum ibid.* **119** (2017) 119901] [arXiv:1601.04339] [INSPIRE].

[139] J. Hisano, D. Kobayashi, W. Kuramoto and T. Kuwahara, *Nucleon electric dipole moments in high-scale supersymmetric models*, *JHEP* **11** (2015) 085 [arXiv:1507.05836] [INSPIRE].

[140] J.R. Ellis, J.S. Lee and A. Pilaftsis, *Electric dipole moments in the MSSM reloaded*, *JHEP* **10** (2008) 049 [arXiv:0808.1819] [INSPIRE].

[141] J. Ellis, J.S. Lee and A. Pilaftsis, *Maximal electric dipole moments of nuclei with enhanced Schiff moments*, *JHEP* **02** (2011) 045 [arXiv:1101.3529] [INSPIRE].

[142] K. Cheung, J.S. Lee, E. Senaha and P.-Y. Tseng, *Confronting higgcision with electric dipole moments*, *JHEP* **06** (2014) 149 [arXiv:1403.4775] [INSPIRE].

[143] S. Hacıömeroğlu and Y.K. Semertzidis, *Hybrid ring design in the storage-ring proton electric dipole moment experiment*, *Phys. Rev. Accel. Beams* **22** (2019) 034001 [arXiv:1806.09319] [INSPIRE].

[144] V. Anastassopoulos et al., *A storage ring experiment to detect a proton electric dipole moment*, *Rev. Sci. Instrum.* **87** (2016) 115116 [arXiv:1502.04317] [INSPIRE].

[145] CMS collaboration, *Search for beyond the Standard Model Higgs bosons decaying into a* $b\bar{b}$ *pair in pp collisions at* $\sqrt{s} = 13$ *TeV*, *JHEP* **08** (2018) 113 [arXiv:1805.12191] [INSPIRE].

[146] ATLAS collaboration, *Search for heavy neutral Higgs bosons produced in association with b-quarks and decaying to b-quarks at* $\sqrt{s} = 13$ *TeV with the ATLAS detector*, Tech. Rep. ATLAS-CONF-2019-010, CERN, Geneva, Switzerland (2019).

[147] ATLAS collaboration, *Search for charged Higgs bosons decaying into top and bottom quarks at* $\sqrt{s} = 13$ *TeV with the ATLAS detector*, *JHEP* **11** (2018) 085 [arXiv:1808.03599] [INSPIRE].

[148] CMS collaboration, *Search for a charged Higgs boson decaying into top and bottom quarks in events with electrons or muons in proton-proton collisions at* $\sqrt{s} = 13$ *TeV*, *JHEP* **01** (2020) 096 [arXiv:1908.09206] [INSPIRE].

[149] CMS collaboration, *Search for charged Higgs bosons decaying into a top and a bottom quark in the all-jet final state of pp collisions at* $\sqrt{s} = 13$ *TeV*, *JHEP* **07** (2020) 126 [arXiv:2001.07763] [INSPIRE].

[150] J. Alwall et al., *The automated computation of tree-level and next-to-leading order differential cross sections, and their matching to parton shower simulations*, *JHEP* **07** (2014) 079 [arXiv:1405.0301] [INSPIRE].

[151] NNPDF collaboration, *Parton distributions with QED corrections*, *Nucl. Phys. B* **877** (2013) 290 [arXiv:1308.0598] [INSPIRE].

[152] A. Alloul, N.D. Christensen, C. Degrande, C. Duhr and B. Fuks, *FeynRules* 2.0 — *a complete toolbox for tree-level phenomenology*, *Comput. Phys. Commun.* **185** (2014) 2250 [arXiv:1310.1921] [INSPIRE].

[153] CMS collaboration, *Search for production of four top quarks in final states with same-sign or multiple leptons in proton-proton collisions at* $\sqrt{s} = 13$ *TeV*, *Eur. Phys. J. C* **80** (2020) 75 [arXiv:1908.06463] [INSPIRE].

[154] T. Sjöstrand, S. Mrenna and P.Z. Skands, *PYTHIA* 6.4 *physics and manual*, *JHEP* **05** (2006) 026 [hep-ph/0603175] [INSPIRE].

[155] DELPHES 3 collaboration, *DELPHES* 3, *a modular framework for fast simulation of a generic collider experiment*, *JHEP* **02** (2014) 057 [arXiv:1307.6346] [INSPIRE].

[156] M.L. Mangano, M. Moretti, F. Piccinini and M. Treccani, *Matching matrix elements and shower evolution for top-quark production in hadronic collisions*, *JHEP* **01** (2007) 013 [hep-ph/0611129] [INSPIRE].

[157] J. Alwall et al., *Comparative study of various algorithms for the merging of parton showers and matrix elements in hadronic collisions*, *Eur. Phys. J. C* **53** (2008) 473 [arXiv:0706.2569] [INSPIRE].

[158] *ATLAS-CMS recommended $t\bar{t}$ cross section predictions webpage*, https://twiki.cern.ch/twiki/bin/view/LHCPhysics/TtbarNNLO.

[159] N. Kidonakis, *Two-loop soft anomalous dimensions for single top quark associated production with a W^- or H^-*, *Phys. Rev. D* **82** (2010) 054018 [arXiv:1005.4451] [INSPIRE].

[160] Y. Li and F. Petriello, *Combining QCD and electroweak corrections to dilepton production in FEWZ*, *Phys. Rev. D* **86** (2012) 094034 [arXiv:1208.5967] [INSPIRE].

[161] W.-S. Hou, M. Kohda and T. Modak, *Search for tZ' associated production induced by tcZ' couplings at the LHC*, *Phys. Rev. D* **96** (2017) 015037 [arXiv:1702.07275] [INSPIRE].

[162] J. Campbell, R.K. Ellis and R. Röntsch, *Single top production in association with a Z boson at the LHC*, *Phys. Rev. D* **87** (2013) 114006 [arXiv:1302.3856] [INSPIRE].

[163] *SM Higgs production cross sections at $\sqrt{s} = 14$ TeV webpage*, https://twiki.cern.ch/twiki/bin/view/LHCPhysics/CERNYellowReportPageAt14TeV2010.

[164] J.M. Campbell and R. Ellis, *$t\bar{t}W^\pm$ production and decay at NLO*, *JHEP* **07** (2012) 052 [arXiv:1204.5678] [INSPIRE].

[165] M. Grazzini, S. Kallweit, D. Rathlev and M. Wiesemann, *$W^\pm Z$ production at hadron colliders in NNLO QCD*, *Phys. Lett. B* **761** (2016) 179 [arXiv:1604.08576] [INSPIRE].

[166] *ATLAS-CMS recommended predictions for single-top cross sections using the Hathor v2.1 program webpage*, https://twiki.cern.ch/twiki/bin/view/LHCPhysics/SingleTopRefXsec.

[167] G. Cowan, K. Cranmer, E. Gross and O. Vitells, *Asymptotic formulae for likelihood-based tests of new physics*, *Eur. Phys. J. C* **71** (2011) 1554 [*Erratum ibid.* **73** (2013) 2501] [arXiv:1007.1727] [INSPIRE].

[168] W.-S. Hou, M. Kohda and T. Modak, *Constraining a lighter exotic scalar via same-sign top*, *Phys. Lett. B* **786** (2018) 212 [arXiv:1808.00333] [INSPIRE].

[169] W.-S. Hou, G.-L. Lin, C.-Y. Ma and C.P. Yuan, *Probing flavor changing neutral Higgs couplings at LHC*, *Phys. Lett. B* **409** (1997) 344 [hep-ph/9702260] [INSPIRE].

[170] S. Iguro and K. Tobe, *$R(D^{(*)})$ in a general two Higgs doublet model*, *Nucl. Phys. B* **925** (2017) 560 [arXiv:1708.06176] [INSPIRE].

[171] W. Altmannshofer, J. Eby, S. Gori, M. Lotito, M. Martone and D. Tuckler, *Collider signatures of flavorful Higgs bosons*, *Phys. Rev. D* **94** (2016) 115032 [arXiv:1610.02398] [INSPIRE].

[172] W. Altmannshofer, B. Maddock and D. Tuckler, *Rare top decays as probes of flavorful Higgs bosons*, *Phys. Rev. D* **100** (2019) 015003 [arXiv:1904.10956] [INSPIRE].

[173] S. Gori, C. Grojean, A. Juste and A. Paul, *Heavy Higgs searches: flavour matters*, *JHEP* **01** (2018) 108 [arXiv:1710.03752] [INSPIRE].

[174] W.-S. Hou, M. Kohda and T. Modak, *Probing for extra top Yukawa couplings in light of $t\bar{t}h$(125) observation*, *Phys. Rev. D* **98** (2018) 075007 [arXiv:1806.06018] [INSPIRE].

[175] BELLE-II collaboration, *The Belle II physics book*, *PTEP* **2019** (2019) 123C01 [*Erratum ibid.* **2020** (2020) 029201] [arXiv:1808.10567] [INSPIRE].

[176] C.-H. Chen and T. Nomura, *Charged Higgs boson contribution to $B_q^- \to \ell\bar{\nu}$ and $\bar{B} \to (P, V)\ell\bar{\nu}$ in a generic two-Higgs doublet model*, *Phys. Rev. D* **98** (2018) 095007 [arXiv:1803.00171] [INSPIRE].

[177] W.-S. Hou, M. Kohda and T. Modak, *Unraveling the couplings of a Drell-Yan produced Z' with heavy-flavor tagging*, *Phys. Rev. D* **98** (2018) 015002 [arXiv:1801.02579] [INSPIRE].

[178] J.M. Campbell, R. Ellis, F. Maltoni and S. Willenbrock, *Higgs-boson production in association with a single bottom quark*, *Phys. Rev. D* **67** (2003) 095002 [hep-ph/0204093] [INSPIRE].

[179] D. Dicus, T. Stelzer, Z. Sullivan and S. Willenbrock, *Higgs boson production in association with bottom quarks at next-to-leading order*, *Phys. Rev. D* **59** (1999) 094016 [hep-ph/9811492] [INSPIRE].

[180] F. Maltoni, T. McElmurry and S. Willenbrock, *Inclusive production of a Higgs or Z boson in association with heavy quarks*, *Phys. Rev. D* **72** (2005) 074024 [hep-ph/0505014] [INSPIRE].

[181] R.V. Harlander and W.B. Kilgore, *Higgs boson production in bottom quark fusion at next-to-next-to leading order*, *Phys. Rev. D* **68** (2003) 013001 [hep-ph/0304035] [INSPIRE].

[182] F. Maltoni, Z. Sullivan and S. Willenbrock, *Higgs-boson production via bottom-quark fusion*, *Phys. Rev. D* **67** (2003) 093005 [hep-ph/0301033] [INSPIRE].

[183] J. Pumplin, D.R. Stump, J. Huston, H.L. Lai, P.M. Nadolsky and W.K. Tung, *New generation of parton distributions with uncertainties from global QCD analysis*, *JHEP* **07** (2002) 012 [hep-ph/0201195] [INSPIRE].

[184] F. Maltoni, G. Ridolfi and M. Ubiali, *b-initiated processes at the LHC: a reappraisal*, *JHEP* **07** (2012) 022 [*Erratum ibid.* **04** (2013) 095] [arXiv:1203.6393] [INSPIRE].

[185] J. Butterworth et al., *PDF4LHC recommendations for LHC run II*, *J. Phys. G* **43** (2016) 023001 [arXiv:1510.03865] [INSPIRE].